Applied Energy 351 (2023) 121809

Contents lists available at ScienceDirect

Applied Energy

journal homepage: www.elsevier.com/locate/apenergy

Methodology for energy management strategies design based on predictive control techniques for smart grids

A. Pajares [a,*], F.J. Vivas [b], X. Blasco [a], J.M. Herrero [a], F. Segura [b], J.M. Andújar [b]

[a] Instituto Universitario de Automática e Informática Industrial, Universitat Politècnica de València, Valencia, Spain
[b] Centro de Investigación en Tecnología, Energía y Sostenibilidad (CITES), Universidad de Huelva, Spain

HIGHLIGHTS

- Microgrids based on renewable energies are a topic of growing interest today.
- The EMS is crucial in microgrids, many authors designed an EMS for a microgrid.
- There is a lack of systematization of this process, from modelling to EMS design.
- This article develops a complete standard methodology for MPC-based EMS design.
- The methodology has been tested and validated in different microgrid architectures.

GRAPHICAL ABSTRACT

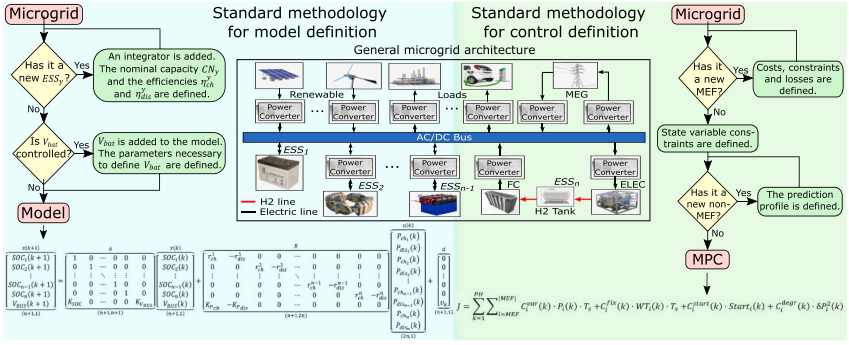

ARTICLE INFO

Keywords:
Model predictive controller
Energy management system
Renewable microgrids
Hydrogen-hybridized backup systems

ABSTRACT

This article focuses on the development of a general energy management system (EMS) design methodology using on model-based predictive control (MPC) for the control and management of microgrids. Different MPC-based EMS for microgrids have been defined in the literature; however, there is a lack of generality in the proposed that would facilitate adapting to new architectures, energy storage system technology, nature of the bus, application, or purpose. To fill this gap, a novel general formulation that is parameterizable, simple, easily interpretable, and reproducible in different microgrid architectures is presented. This is the result of the development of a novel methodology, which is also presented. It considers the state space formulation of the controller from the initial modelling phase, from the dynamics of the energy storage systems represented by their models to the subsequent definition of the optimisation problem. This is developed through the design of the general cost function and the formulation of constrains, by means of general guidelines and reference values. To evaluate the performance of the developed methodology, simulation tests were carried out for four different microgrid architectures, with different applications and objectives, also considering different generation conditions, demand profiles, and initial conditions. The results showed that, with some simple guidelines and regardless of the case study, the developed MPC controller design methodology can address the technical-economic optimisation problem associated with energy management in microgrids in an easy and intuitive way.

* Corresponding author.
E-mail address: alpafer1@upv.es (A. Pajares).

https://doi.org/10.1016/j.apenergy.2023.121809
Received 17 May 2023; Received in revised form 3 August 2023; Accepted 19 August 2023
Available online 7 September 2023

Acronyms

BoP	Balance of plant
BSS	Battery-based storage system
DG	Diesel generator
ELEC	Electrolyser
EMS	Energy management system
ESS	Energy storage system
EV	Electric vehicle
FC	Fuel cell
HBSS	Hydrogen-based storage system
HESS	Hybrid energy storage system
LTI	Linear time invariant
MEG	Main electrical grid
MEF	Manipulable energy flow
MPC	Model-based predictive control
non-MEF	Non-manipulable energy flow
non-MEF-	Non-manipulable energy flow injected to the bus
non-MEF+	Non-manipulable energy flow extracted from the bus
O&M	Operation and maintenance
P2P	Peer-to-peer
PV	Photovoltaic
SCB	Supercapacitor bank
SMES	Superconducting Magnetic Energy Storage
SOC	State of charge

Symbols

C_i^{var}	Variable cost MEF_i $(€/Wh)$
C_i^{fix}	Fixed cost MEF_i $(€/h)$
C_i^{start}	Start cost MEF_i $(€)$
C_i^{degr}	Degradation cost MEF_i $(€/W^2)$
CN_j	Energy capacity of ESS_j (Wh)
ESS_j	Energy storage system $(j = \{1,\ldots,n\})$
$\overline{H}$ / $\underline{H}$	Maximum and minimum value of variable H (H = $\{x_l, P_i, \Delta P_i\}$)
K_{Pch}/K_{Pdis}	Coef. to battery related to charge/disc. power (V/W)
K_{SOC}	Coef. to battery related to SOC $(V/\%)$
$K_{V_{BUS}}$	Coef. to battery related to V_{BUS}
$Loss$	Total losses of the microgrid (W)
$Loss_i$	Variable losses depending on the power of MEF_i
$Loss_i^{BoP}$	Balance of plant MEF_i (W)
n	Number of ESS systems
$N_{els/fc}$	Case 4, number of active ELECs and FCs (integer)
MEF_i	Manipulable energy flow $(i = \{ch_1, dis_1, \ldots, ch_n, dis_n, gridin, gridout\})$
P_i	MEF_i power (W)
P_{nMEF-}	Total power non-MEF supplied by the microgrid (W)
P_{nMEF+}	Total power non-MEF injected into the microgrid (W)
P_{load}	Load power (W)
P_{EV}	Electric vehicle power (W)
P_{HA}	House appliance power (W)
P_{HVAC}	Heat., ven., and air con. power (W)
P_{ren}	Renewable power (W)
P_{PV}	Photovoltaic power (W)
P_W	Wind turbine power (W)
PH	Prediction horizon (h)
$r_{ch/dis}^j$	Charge/discharge ratio ESS_j $(\%/W)$
SOC_j	State of charge of ESS_j $(\%)$
$SOC_j^{ini/end}$	Initial and final state of charge of ESS_j $(\%)$
$Start_i$	Start MEF_i (binary)
T_s	Sample time (h)
V_{BUS}	DC bus voltage (V)
V_{BUS}^{ini}	Initial DC bus voltage (V)
WT_i	Working time MEF_i (binary)
$x(k)$	State variable $(SOC_1,\ldots,SOC_n, V_{BUS})$
ΔP_i	MEF_i power variation (W)
δP_i	MEF_i increment power without on and/or off process (W)
$\eta_{ch/dis}^j$	Charge/discharge efficiency ESS_j $(\%)$
v_k	Independent term related to V_{BUS} model (V)

1. Introduction

A smart grid is a microgrid, formed by electrical generation sources, mainly renewable, an energy storage system (ESS), as well as a set of loads, and depending on the topology, the connection to the main electrical grid (MEG) [1]. The concept of smart grid intrinsically includes the word "intelligence", so it is a microgrid that incorporates local control algorithms, as well as supervision, which allow guaranteeing the correct and optimal operation of each equipment [1].

Despite the benefits of the use of smart grids, there are currently a series of technical problems associated with the technology that need to be solved or mitigated so that they can be considered as a viable and competitive solution with respect to the current energy model [1]. In this sense, the stochasticity in the generation of renewable energy sources requires the use of energy storage system (ESS) that guarantee the energy balance in the case of energy mismatch between generation and demand [1].

Regarding ESSs, different technologies can be found such as battery energy storage systems (BSSs), supercapacitor energy storage systems (SCBs), hydrogen-based energy storage systems (HBSSs) or diesel generators (DGs), among others, as well as architectures, based on a single ESS or hybrid energy storage system (HESS) [2,3]. Despite the benefits of each technology, there are a number of technological problems related to the operating conditions, such as: the integration and management of the charging and discharging process of BSS/SCB, especially in topologies where the DC bus relies on their direct connection [4], the crossover effect or slow operating dynamics in electrolysers (ELECs) [1], as well as the electrochemical degradation during the cycles and hours of operation of fuel cells (FCs) [5] or the CO_2 emissions in DGs [1].

To ensure the correct operation of smart grids, considering the design criteria, operating constraints, and technical problems to be solved, it is necessary to use energy management strategies (EMSs) [1]. This type of strategies has the function of defining which element, at what time and under what operating conditions will act according to technical and economic optimisation criteria, including parameters such as degradation, performance, load management, operation and maintenance cost, etc. Thus, the range of problems to be addressed by the microgrid control system is very broad.

In terms of EMS, in the last decade the use of techniques based on optimal control has proliferated. This type of solution allows a multi-objective optimisation problem to be posed by defining a cost function to be minimised [6]. The resolution of the proposed control problem always allows guaranteeing the maximum utilisation of the energy resource, as well as optimising the system response according to the energy situation and state of the equipment.

For implementation, although there are many optimisation techniques that can be used for microgrid control, model-based predictive control (MPC) provides a general framework for solving most problems using some common ideas in an integrated way. MPC can respond to optimal control problems in multivariable systems subject to constraints

and disturbances, proposing a closed-loop control structure based on the concept of receding horizon [7]. This type of strategy allows the implementation of an on-line optimisation algorithm based on the current system parameters, the model and their short-term prediction, defined by the prediction horizon (PH) [8]. In this sense, the incorporation of the future behaviour of the system is of crucial importance to optimise the use of microgrids [9].

The idea of applying MPC-based EMS is not new, in fact different MPC algorithms have been successfully tested in multiple microgrid architectures and applications [10]. However, the main problem lies in the lack of generality of the different formulations to be adapted to new architectures, ESSs or targets, in order to enhance the use of microgrids in multiple domains and scales. To systematise the review of the different MPC-based EMSs, the different works have been classified according to the optimisation problem posed, Tracking MPC and Economic MPC.

Tracking MPC proposes an optimisation problem that poses a state vector reference tracking problem to establish certain recommended operating conditions, while aiming to guarantee the power balance.

Clear examples of these solutions are evaluated in [11–13] for renewable microgrids with HESS based on multiple BSSs and HBSSs over a DC bus modelled using hybrid linear time invariant (LTI) models. In particular, [11] proposes the use of an event-based Tracking MPC with several LTI-type models and pre-designed cost functions to increase the performance of the controller depending on the value of the state vector for office-type application. On the other hand, [12,13] propose a single MPC Tracking for use in stand-alone and grid-tie residential applications respectively. Regardless of the solution adopted, a weighted cost function is proposed for the tracking of reference values for SOC_{bat} and SOC_{H2} considered optimal. The determination of these values does not respond to an analytical optimisation process but is carried out by means of previous simulations for different generation and consumption profiles and initial conditions in the microgrid under study. A more general solution is presented in [14], where a renewable microgrid model with HESS based on HBSS and BSS with direct connection to the DC bus is used. A general LTI model and weighted cost function are presented that integrates technical (SOC_{bat} and SOC_{H2} reference tracking, bus voltage control, degradation minimisation, etc.) and economic (minimisation of the MEG power purchase/sale cost) objectives by proposing a hybrid Tracking and Economic MPC for short- and long-term optimisation of the microgrid. Despite its attempts to present a general problem, the parameter tuning process is based on heuristic rules implemented by a fuzzy controller.

Even with proven performance, Tracking MPC-based EMSs define a multi-objective problem based on a particular weighted cost function, in which these weighting factors are often not easily interpretable, as they are not directly related to physical variables [15]. This means that their tune is complex, requiring a general tuning based on heuristic techniques, which leads to a loss of generality in their design [15].

In order to make the optimisation problem more interpretable, the Economic MPC translates the control problem into a cost optimisation problem [16]. This allows the cost function to include only monetary cost terms, which makes it interpretable and at the same time homogenizes and standardises all the objectives to be achieved around the cost variable [16]. Thus, several works address the control problem based on Economic MPC for various microgrid architectures and applications.

In [17,18] the use of an Economic MPC based on a hybrid LTI model is proposed for the management of an isolated microgrid with a HESS based on BSS and HBSS. The proposed cost function integrates variable costs for each ESS_j linked to operation and maintenance (O&M) and depreciation costs for long-term system optimisation. Similarly, the use of an Economic MPC for the management of a distribution network based on microgrids with renewable generation and HESS based on BSS and microturbines is proposed in [19]. The proposed cost function integrates variable costs linked to the operating costs of the HESS and the energy flows between the different microgrids with the aim of guaranteeing a zero external energy balance of the distribution network. A more complex problem is addressed in [20]. In this case, the use of an Economic MPC is proposed for the optimal management of a DC microgrid with possible connection to the MEG, with multiple generation systems, renewable and non-renewable, and a HESS composed of BSS, SCB, microturbines and DG. The cost function has been designed to minimise the variable costs linked to the operating costs of the HESS, the costs linked to interruptions in the power supply to the demand (when operate in isolated-mode) and the net CO_2 emissions of the microgrid.

Again, despite the excellent results, these works lack the generality required for their correct application in microgrids with different architectures and topologies. Thus, to solve this shortcoming, few works focused their efforts to try to present a general methodology for the design of EMS based on Economic MPC, from the modelling phase to the subsequent definition of the cost function and constraints.

A first approach is presented in [20], which lays the foundations for the design of general EMSs based on Economic Distributed MPC. In particular, it establishes the design of general hybrid LTI-type models for a general microgrid architecture (with AC or DC bus) whose state variables are defined by its ESSs. Similarly, the optimisation problem is established by defining different cost functions and constraints depending on the type of application, connection to the MEG and type of generation, renewable or non-renewable. In view of the above, the definition of the cost function is not universal and therefore the proposed methodology cannot be considered fully general. Something similar happens in the general methodology proposals presented in [21,22]. Unlike the previous work, these works consider a certain renewable DC microgrid architecture based on a HESS formed by BSS and HBSS. The innovation is based on the design and validation of general cost functions adapted to the proposed microgrid architecture for its correct management in applications linked to the daily and intraday market, peer-to-peer (P2P) as well as for electricity market regulation services. Again, these formulations lack generality as they only allow a restricted parameterisation of the problem either to the model or the cost function.

From the literature review it can be deduced that the design of MPC-based EMS has grown exponentially in the last decade and is presented as a very powerful tool for the control of microgrids with very complex architectures in very demanding applications. However, there is a clear trend towards the design of very efficient and increasingly powerful control algorithms and models, but at the same time specific to a given microgrid architecture or application. Logically, this gives a lack of flexibility and generality to the algorithm, and therefore puts at risk the replicability of these techniques in other microgrid architectures and applications.

In this sense, the formulation of a general MPC-based EMS must consider all the variables necessary for its definition. These include the architecture of the microgrid, the ESSs used, the connection to the MEG, the nature and method of DC bus integration (by power converter or direct connection of ESSs), as well as the constraints and the problem to be optimised, the minimisation of O&M and MEG costs, the control of DC bus voltage, the increase of ESS lifetime, etc. Based on the above, it is necessary to systematise and facilitate their application at different stages (model, optimisation problem, cost function, etc.), especially regarding the cost function to be optimised.

On the basis of the analysis carried out, the main contributions of the paper can be summarised as follows:

- Development of a standard methodology for the design of a control-oriented state space model for smart grids. This methodology is applicable regardless of its architecture, the ESS system, the nature of the internal bus, AC or DC, and its connection to the ESS, by power converter or direct connection.
- Development of a general EMS-based MPC methodology (with economic optimisation), which is parameterizable, simple to implement, easily interpretable and reproducible for different microgrids. This

Table 1
Summary of MPC-based modelling and EMS solutions found in the literature compared to the authors' proposal.

	Microgrid Architecture and Model		MPC-based EMS			
Ref.	General development	Bus Topology	General development	DC Bus voltage control	Parameterization	Multi-application validation
[11–13]	State-Space Hybrid LTI model	DC bus	Tracking MPC	No	No	No Residential and office-type application
[14]	State-Space LTI model	DC bus and ESS-supported DC bus	Tracking MPC	Yes	Yes Model, cost function and weighting factors	No Residential application
[17,18,20]	State-Space Hybrid LTI model	DC bus	Economic MPC Cost index	No	No	No Residential application
[19]	State-Space Hybrid LTI model	AC bus	Economic MPC Cost index	No	No	No Distribution network application
[20]	State-Space Hybrid LTI model	AC bus and DC bus	Economic MPC Cost index	No	Yes Model cost index and constraints (Restricted parameterisation)	No Secondary regulation
[21,22]	State-Space Hybrid LTI model	DC bus	Economic MPC Cost index	No	Yes Model cost index and constraints (Restricted parameterisation)	Yes Primary regulation Secondary regulation P2P
Authors's approach	State-Space Hybrid LTI model	AC bus, DC bus and ESS-supported DC bus	Economic MPC Cost index	Yes	Yes Model, cost index and constraints	Yes Residential application EV charging application Industrial application Secondary regulation

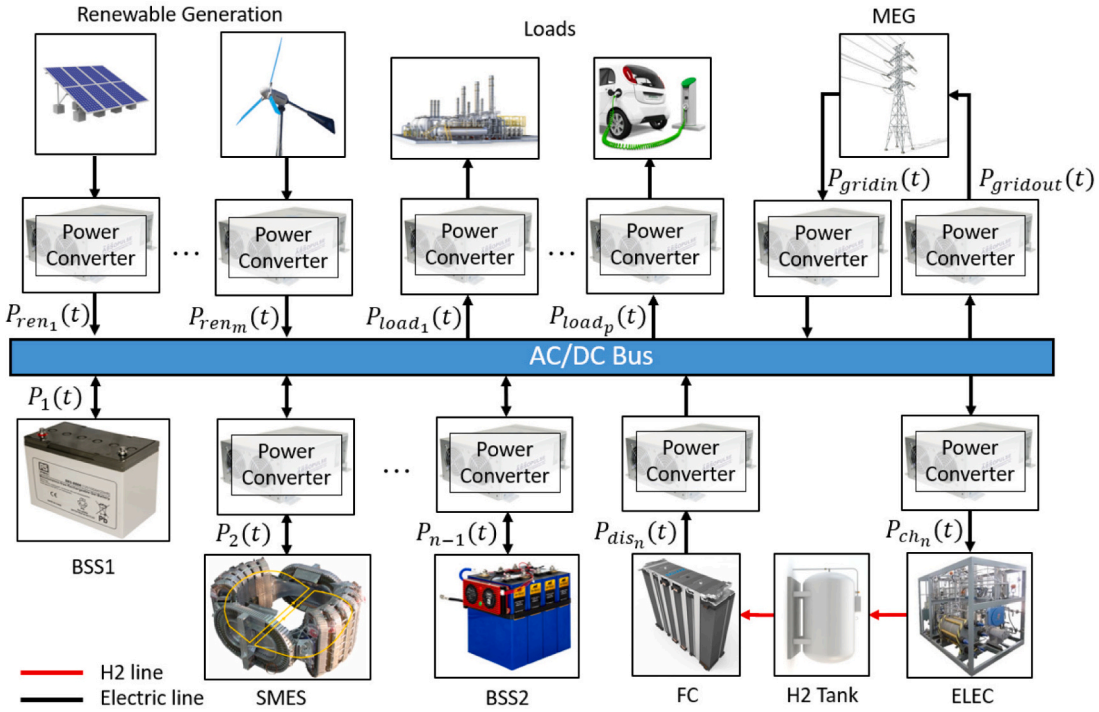

Fig. 1. Example of general microgrid architecture with multiple ESSs.

methodology applies regardless of application, scale, architecture (with or without ESS-supported DC bus), or microgrid configuration.
- The applicability and generality of the developed methodology has been tested and validated in different case studies for different scales, architectures and microgrid applications.

Finally, to highlight the novelty of this research, Table 1 summarises its main characteristics in comparison with the analysed literature.

The rest of the article is organised as follows. Section 2 describes the proposed methodology for general microgrid modelling considering its architecture and integration method. Section 3 develops the general formulation of the MPC-based EMS. Section 4 performs the validation of the proposed modelling and EMS design methodology and discusses the results for four different microgrids architectures and applications under study. Finally, Section 5 presents the main conclusions and future lines of work.

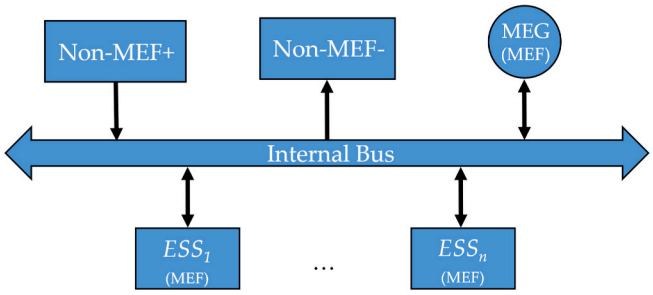

Fig. 2. Generic microgrid architecture.

2. Microgrid model

2.1. Microgrid architecture

To implement a general model for the development of MPC-based EMSs, a microgrid with a general architecture is considered for the modelling process (see Fig. 1). This architecture can characterise many microgrids, regardless of the energy sources, renewable or non-renewable, the system loads, the ESSs used, the connection or not to the MEG, the nature and method of bus connection, etc. In microgrid architectures whose DC bus relies on the direct connection of ESSs, it is assumed that, at most, a single ESS is directly connected to the bus [23].

Regardless of the architecture and nature of the constituent elements of the microgrid under study, to guarantee the generality of the model, a homogenisation is required in the definition of the dynamics of each element with respect to a common variable, in this case, with respect to the power or electrical energy. Therefore, each element, and ultimately the microgrid, can be modelled according to the energy flows that each element exchanges with the bus in each sampling period.

Obviously, some of these energy flows can be manipulable (MEF) and others non-manipulable (non-MEF).

On the one hand, non-MEFs are defined as energy flows that a priori are not controllable, or whose control is partial or limited, as in the case of local controllers oriented to maximise the use of renewable energy generation. The values of these powers in the optimisation process are assigned by predictions. Non-MEFs will be classified according to whether they are demanded from the microgrid (non-MEF-, for example, the power of loads) or supplied to the microgrid (non-MEF+, e.g., power generated from renewable energy sources).

On the other hand, MEFs guarantee the power and energy balance in the bus in the face of mismatches between generation and demand, and, therefore, provide certain degrees of freedom in the optimisation of the energy management problem. The EMS calculates the powers of the MEFs. Therefore, MEFs will be given by the charging or discharging processes of the ESSs (batteries, supercapacitors, HBSS, etc), and the use of the MEG, when considering a grid-connected architecture.

Based on the above, any microgrid architecture, regardless of its complexity, can be represented as a set of MEFs (associated with ESSs and MEG) and non-MEFs (associated loads and renewable generation), as shown in Fig. 2. This will be the starting point for the definition of the microgrid model in the next sections.

2.2. Modelling

Once the generic architecture has been defined, Fig. 2, it is necessary to define the microgrid model, which must satisfy certain requirements of accuracy and computability to favour its application in real microgrids.

In view of the above requirements, although a nonlinear model allows, a priori, to obtain a more accurate model of the dynamics of the microgrid, given that most of its constituent elements have a nonlinear behaviour, this can turn the optimisation problem into a very complex problem, especially if it is considered that the microgrid can be defined by a very complex architecture [14]. Therefore, the design of EMS based on this type of model requires algorithms specially designed to address nonlinear optimisation problems, which, depending on the nonlinear nature of the model, can make the optimisation problem unsolvable or computationally intractable for the design of online MPC control strategies [24].

On the other hand, although the use of linear LTI models facilitates their computation, since they allow implementing linear control theory, they can present a low accuracy, since the dynamics or behaviour of the ESSs during the charge and discharge processes is different, for example, different charge and discharge performances in batteries, different dynamics and operation of ELECs and FCs in HBSSs, etc.

Therefore, it is necessary to transform or adapt the above modelling option so that it can be used in the control strategy. Thus, the proposed alternative is based on approximating the nonlinear model by a piecewise linear model in which the behaviour of the different MEF_j can be separated depending on the direction of the power flows. For this reason, the charging power (P_{ch_j}) and discharging power (P_{dis_j}) of all ESS_j are unfolded as $P_j = P_{dis_j} - P_{ch_j}$, as well as the power purchase (P_{gridin}) and sale ($P_{gridout}$) of energy to the MEG as $P_{grid} = P_{gridin} - P_{gridout}$.

Based on the proposed modelling philosophy, the following sections will present the methodology for obtaining the general model of the microgrid, based on the modelling of the ESSs of the microgrid, the DC bus voltage (V_{BUS}), when its control is necessary, and finally, the bus power balance, which governs the operation of the microgrid, independent of its connection to the MEG.

2.2.1. Energy storage system

Currently, there are different ESS technologies for use in microgrids, in particular, ESSs defined by different battery technologies, supercapacitors, magnetic superconductors, HBSSs, compressed air systems, etc., have been reported in the scientific literature. Regardless of the technology, their dynamics can be defined as a discrete-time first-order integrator with respect to state of charge (SOC) according to (1), [25].

$$SOC_j(k+1) = SOC_j(k) + \frac{\eta^j(k)\cdot T_s}{CN_j} P_j(k) \tag{1}$$

Where η^j, CN_j and P_j are the efficiency, rated capacity, and power of the ESS_j respectively and T_s is the sample time.

According to the modelling criterion based on piecewise linear model, in all ESSs the MEFs are unfolded depending on the energy flow direction. Thus, the power of any ESS is obtained from the combination of the power of the different MEFs: $P_j = P_{dis_j} - P_{ch_j}$. Since these MEFs can be mutually exclusive, binary variables, and constraints must be added in the MPC definition to avoid both operating simultaneously (see Section 3.2). Thus, if ESS_j is in charging mode: $P_{ch_j} \geq 0$ and $P_{dis_j} = 0$, and, on the other hand, if ESS_j is in discharging mode: $P_{dis_j} \geq 0$ and $P_{ch_j} = 0$. Similarly, if it is considered, in general, that the performance of the charging and discharging process, η^j_{ch} and η^j_{dis} respectively, are different, Eq. (1) can be described according to (2), [9].

$$SOC_j(k+1) = SOC_j(k) + r^j_{ch}\cdot P_{ch_j}(k) - r^j_{dis}\cdot P_{dis_j}(k) \tag{2}$$

Where the charging and discharging ratios for each ESS_j, r^j_{ch} and r^j_{dis} respectively, are defined in (3).

$$r^j_{ch} = \frac{\eta^j_{ch}}{CN_j}\cdot T_s; r^j_{dis} = \frac{1}{\eta^j_{dis}\cdot CN_j}\cdot T_s \tag{3}$$

2.2.2. Direct current bus voltage

Considering the generality of the proposed model, there are microgrids with DC buses supported by the direct connection (without the use of a power converter) of an ESS, usually a BSS and/or a SCB [23] (see ESS_1 in Fig. 1). This particular type of microgrids require DC bus voltage

control, with the objective of guaranteeing an operating voltage range for the microgrid interconnection, while performing the ESS charging and discharging process correctly, safely and with the least possible negative impact in terms of degradation [4].

Thus, when it is desired to manage this type of microgrids, it must be considered that, in the absence of a power converter, the ESS power, and secondly, the bus voltage, cannot be imposed directly. However, the imposition of power setpoints of the rest of the ESSs and MEGs, and the guarantee at all times of the power balance, indirectly leads to the definition of the ESS power and voltage setpoints.

In view of the above, for the management of this type of topologies, it is important to have the bus voltage (V_{BUS}) to proceed to its control, for example, by setting equality or inequalities constraints to keep the voltage between maximum and minimum limits.

For V_{BUS} modelling, there are many works in the scientific literature that allow modelling the dynamic voltage behaviour of batteries or supercapacitors [26]. Many of them are nonlinear models, as is the case of the electrochemical models of Tremblay [27] or Copetti [28] for battery voltage modelling. Other examples of control-oriented linear models are based on the use of first- or second-order Thevenin equivalent circuits for modelling both batteries and supercapacitors [26,29,30].

Regardless of the model used, the different formulations allow modelling the voltage dynamics with respect to the stored energy (SOC), the charge or discharge energy, and, depending on the model, the internal temperature [31,32]. In view of the above, if the thermal effect of the models is neglected, and from the development of the differential equations governing linear models, or from the linearization of non-linear models, a general linear V_{BUS} model can be defined according to Eq. (4), [14].

Eq. (4) is formulated from non-linear models that reflect the behaviour of a battery-based energy storage system. Specifically, for a battery, regardless of the technology used, the dynamics of its voltage is given as a function of the SOC, the charging or discharging power, and, logically, if the equation that models it is discrete, the voltage value in the previous sampling period. Since these this type of non-linear models are very complex, require the design of non-linear controllers, and are rarely needed (unless a specific battery test is being performed, in a microgrid, the SOC of the battery-based energy storage system must be kept in a relatively short and controlled range, without large dynamic excursions), the solution adopted has been the use of linear models based on the approximation by means of a first order Taylor polynomial.

Thus, for the case under study, in which the DC bus is supported by the direct connection of a battery bank, its voltage ($V_{BUS}(k+1)$) can be determined from the partial derivatives with respect to $SOC(k)$, $P_{ch}(k)$, $P_{dis}(k)$ and $V_{BUS}(k)$, in the non-linear equation that defines the model. These partial derivatives determine the value of the coefficients $K_{V_{BUS}}$, K_{SOC}, K_{Pch}, K_{Pdis}, and, if applicable, the independent term resulting from the linearisation process, v_k.

In this case, Eq. (4) includes this general linear approximation, which may be obtained from the non-linear model to be applied, depending on the type of battery or application.

$$V_{BUS}(k+1) \approx K_{V_{BUS}} \bullet V_{BUS}(k) + K_{SOC}\cdot SOC_j(k) + K_{Pch}\cdot P_{ch_j}(k) - K_{Pdis}\cdot P_{dis_j}(k) + v_k \tag{4}$$

Where $K_{V_{BUS}}$, K_{SOC}, K_{Pch} and K_{Pdis} are the battery coefficients of V_{BUS}, SOC_j, P_{ch_j} and P_{dis_j} respectively, and v_k is the independent term result of the linearization process.

2.2.3. Power balance

The general architecture of the microgrid is shown in Fig. 2. Regardless of its architecture or complexity, the microgrid must provide the non-manipulable energy flows supplied by the microgrid, i.e., all non-MEF- (e.g., the load power P_{load} cannot be controlled from the microgrid). For this purpose, the microgrid relies on all non-controllable generation units, non-MEFs+, e.g., renewable generation (P_{ren}), as well as the contribution of MEFs, composed of ESSs (P_j), and if applicable, MEG (P_{grid}). Based on the above, if energy conversion and transport losses and auxiliary consumption are considered ($Loss$), the microgrid must satisfy the power balance according to Eq. (5) [9]. Of course, in isolated architectures, P_{grid} term is zero.

According to the established criterium, the powers associated with MEFs ($P_{gridin}, P_{gridout}, P_{ch_j}$ and $P_{dis_j} \forall ESS_j$) and non-MEFs (P_{nMEF+}, P_{nMEF-}) are individually positive. However, for the definition of the power balance, Eq. (5), the powers injecting and extracting power to the microgrid must have opposite sign. Therefore, it has been considered that the powers injected into the DC bus (P_{gridin}, P_{dis_j} and P_{nMEF+}) add up with a positive sign; conversely, the powers extracted from the DC bus ($P_{gridout}, P_{ch_j}$ and P_{nMEF-}) are added with negative sign to the power balance (Eq. (5)). In the case of the MEFs power (P_j and P_{grid}), the sign is determined by the direction of power flow defined above ($P_{grid} = P_{gridin} - P_{gridout}$ and $P_j = P_{dis_j} - P_{ch_j}$, following the same criteria). Of course, in both P_{grid} and P_j it is necessary to prevent the optimisation from proposing a value in the two variables that compose them simultaneously. Restrictions are added to ensure that this cannot happen (please see details in Section 3.2. Restrictions).

Thus, based on (5), when $P_{nMEF+} > P_{nMEF-}$ there is surplus energy in the bus. This surplus energy can be used, regardless of the process, for storage in the ESSs, or to obtain an economic benefit by selling energy to MEG, when possible. On the other hand, when $P_{nMEF+} < P_{nMEF-}$ there is an energy deficit in the bus. This energy deficit can be made up by discharging energy from the ESSs, or by purchasing energy from MEG, when possible.

$$P_{nMEF+} - P_{nMEF-} - Loss(k) + P_{grid}(k) + \sum_{j=1}^{n} P_j(k) = 0 \tag{5}$$

In this case, the $Loss(k)$ term includes all the total losses of the microgrid not previously considered, according to Eq. (6). This term does not include the losses related to the efficiencies in the different ESS_j since they have already been considered in Eq. (2). Similarly, this term will not include the losses related to the non-MEFs, since by considering the net energy flows with respect to the bus (P_{nMEF+} and P_{nMEF-}), these losses have already been considered in the respective non-MEFs+ and non-MEFs- terms.

$$Loss(k) = \sum_{i=MEF}^{|MEF|} Loss_i(k)\cdot P_i(k) + Loss_i^{BoP}\cdot WT_i \tag{6}$$

Where $Loss_i^{BoP}$ and $Loss_i$ are the balance of plant (BoP) and the variable losses of MEF_i respectively, and WT_i is a binary variable defining the working time of MEF_i. The MEF_i can inject ($i = \{dis_1, \ldots, dis_n, gridin\}$) or extract energy ($i = \{ch_1, \ldots, ch_n, gridout\}$) to the microgrid. $WT_i = 1$ if the MEF_i injects or extracts energy, i.e. if it operates; and $WT_i = 0$ if the MEF_i does not inject or does not extract energy, i.e. if it does not operate.

According to Eq. (6), $Loss(k)$ is defined by two types of losses, variable and fixed. Thus, the first term models the variable power losses as a function of the power P_i. These variable losses are associated with the rest of the subsystems that are not modelled, such as the power converters or the power transmission lines and connections. These elements have variable losses as a function of the power consumed or generated

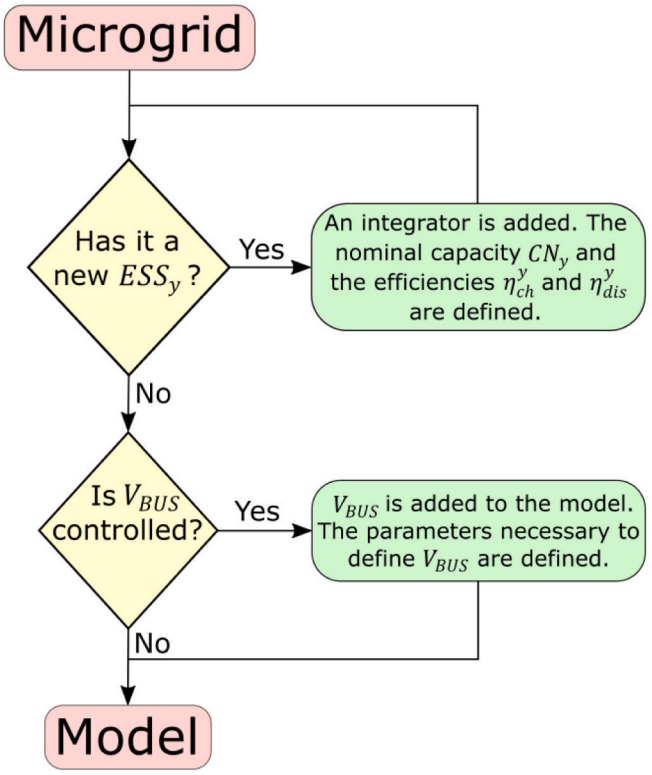

Fig. 3. Flow chart for the definition of the microgrid model.

Table 2
Necessary parameters for the definition of the microgrid model for n ESSs and DC bus supported by ESS.

ESSs Parameters						
	ESS_1				ESS_n	
CN_1	η^1_{ch}	η^1_{dis}	⋯	CN_n	η^n_{ch}	η^n_{dis}
DC bus Parameters (*if* V_{BUS})						
$K_{V_{BUS}}$		K_{SOC}		K_{Pch}	K_{Pdis}	v_k

(2). Therefore, a state-space model is a good alternative for modelling microgrids to be controlled by an MPC. Likewise, due to the generality of the model, V_{BUS} can be integrated in the state vector in those microgrid architectures and applications that require it.

Finally, the outputs will coincide with the states, $y(k) = x(k)$, and the manipulated variables ($u(k)$) will be the charge/discharge powers of each ESS_j ($\left[P_{ch_1}\ P_{dis_1} \ldots P_{ch_n}\ P_{dis_n}\right]^T$).

$$x(k+1) = Ax(k) + Bu(k) + d$$

$$y(k) = x(k) \tag{7}$$

Thus, considering (2)–(4), according to the general expression (7), the general state-space model of any microgrid, with a discrete number n of ESSs, regardless of its architecture, nature of the ESS or bus connection, responds to Eq. (8). In microgrid architectures whose DC bus is supported by the direct connection of ESSs, it is assumed that, at most, a single ESS is directly connected to the bus (ESS_1). Of course, this ordering is not mandatory and, therefore, both the state and input matrix (A and B respectively) can be adapted depending on the position of the ESS supporting the DC bus without no loss of generality.

$$\overbrace{\begin{bmatrix} SOC_1(k+1) \\ \vdots \\ SOC_n(k+1) \\ V_{BUS}(k+1) \end{bmatrix}}^{x(k+1)}_{(n+1,1)} = \overbrace{\begin{bmatrix} 1 & \cdots & 0 & 0 \\ \vdots & \ddots & \vdots & \vdots \\ 0 & \cdots & 1 & 0 \\ K_{SOC} & 0 & \cdots & K_{V_{BUS}} \end{bmatrix}}^{A}_{(n+1,n+1)} \overbrace{\begin{bmatrix} SOC_1(k) \\ \vdots \\ SOC_n(k) \\ V_{BUS}(k) \end{bmatrix}}^{x(k)}_{(n+1,1)} + \overbrace{\begin{bmatrix} r^1_{ch} & -r^1_{dis} & \cdots & 0 & 0 \\ \vdots & \vdots & \ddots & \vdots & \vdots \\ 0 & 0 & \cdots & r^n_{ch} & -r^n_{dis} \\ K_{Pch} & -K_{Pdis} & 0 & \cdots & 0 \end{bmatrix}}^{B}_{(n+1,2n)} \overbrace{\begin{bmatrix} P_{ch_1}(k) \\ P_{dis_1}(k) \\ \vdots \\ P_{ch_n}(k) \\ P_{dis_n}(k) \end{bmatrix}}^{u(k)}_{(2n,1)} + \overbrace{\begin{bmatrix} 0 \\ \vdots \\ 0 \\ v_k \end{bmatrix}}^{d}_{(n+1,1)} \tag{8}$$

by the different devices in the microgrid, in short, these losses depend on the power of the MEFs.

The second term models the fixed losses known as $Loss_i^{BoP}$. These losses are associated with the consumption of auxiliary equipment that must be provided by the microgrid and are required for the correct operation of the MEFs. Perhaps the clearest example of these losses may be the consumption associated with the BoPs of HBSSs. These systems are in turn made up of several subsystems: pumps, controllers, valves, etc., which normally have a fixed energy consumption, independent of the power consumed/generated by the HBSS. Other examples can be considered, such as the consumption of auxiliary monitoring systems for battery management or other ESSs. In view of the above, these losses will only be considered when the MEF_i is providing or generating power ($WT_i = 1$). Otherwise, these losses will be zero ($WT_i = 0$).

2.2.4. Microgrid model

Since the nature of the ESSs represent the dynamic component of the microgrids, their models are generally formulated as state-space equations, according to the general model shown in (7) [9], where the state variables $x(k)$ coincide with the SOC_j of each ESS_j $\left([SOC_1 \ldots SOC_n]^T\right)$, whose behaviour is defined by a first-order integrator according to Eq.

Thus, based on the general formulation (8) and the general architecture defined in Fig. 2, to define the dynamic model of a specific microgrid, the procedure described in Fig. 3 should be followed.

First, the number of ESSs must be identified, and a new integrator must be added to the model for each ESS_j. Likewise, for each ESS_j, its characteristic parameters will be defined according to the model proposed in Table 2. Specifically, for each ESS_j its nominal capacity CN_j (in Wh) and its charging and discharging performances (η^j_{ch} and η^j_{dis} respectively) will be defined, in order to calculate its charging and discharging ratios, r^j_{ch} and r^j_{dis} (according to eq. (3)).

Finally, the bus connection method will be evaluated, and in those cases where the microgrid architecture requires it, V_{BUS} will be integrated as a new state variable in the model. To obtain it, the desired ESS model can be used, requiring the necessary procedures to obtain a linear model according to the general Eq. (4). Similarly, for its formulation, the characteristic parameters will be defined according to the proposed Table 2.

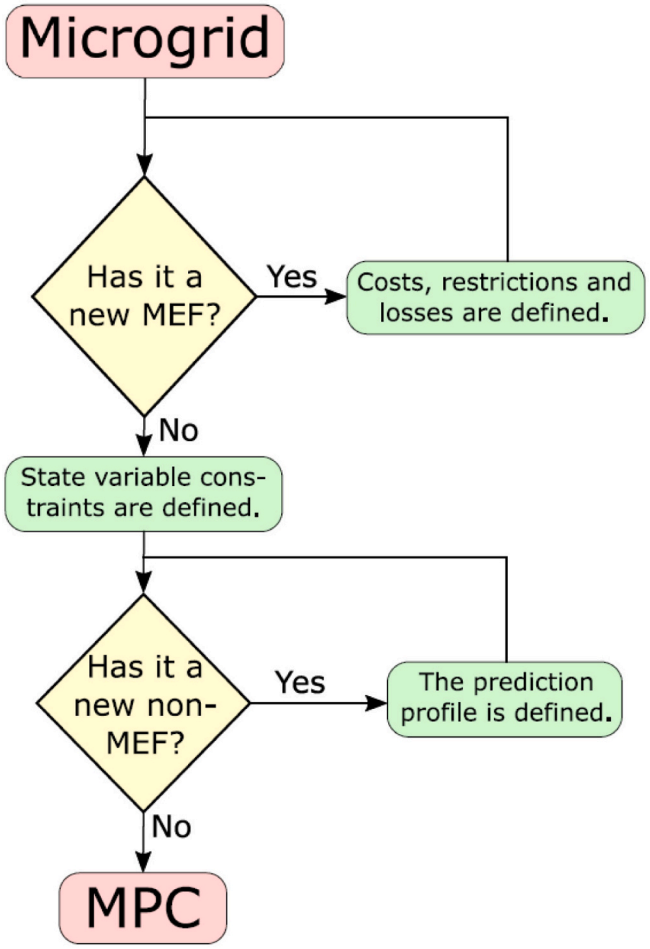

Fig. 4. Flow chart for the definition of the MPC.

3. Model predictive control based energy management system

The EMS decides at all times and based on objectives, the MEF that must be supplied or consumed by the different devices of the microgrid to be managed. In this work, an MPC is proposed for the design of the EMS of a microgrid. The MPC is a strategy based on the optimisation of a cost function, which makes use of a process model and some predictions of the non-MEF to evaluate the effect of the control action on a plant along the prediction horizon.

A widely used approach in the literature for solving an MPC-based EMS, computationally manageable, is the definition of a mixed integer programming (MIP) problem using integer and/or binary variables [33,34]. The inclusion of integer or binary variables allows scenario changes while maintaining simplicity in the model. When these problems have a linear cost function it results in a mixed integer linear programming (MILP) [33,35–37, when they have a quadratic cost function it results in a mixed integer quadratic programming (MIQP) [9,38]. In both cases there are very efficient and consolidated software for its resolution [32].

Therefore, once the model has been defined (see Section 2), to define MPC-based EMS it is necessary to:

- Define a cost function J to be optimised by the MPC.
- Define a prediction horizon PH suitable to optimise energy management and operation of ESS.
- Define the physical and operational constraints of the microgrid.

In an MPC-based EMS, the definition of the cost function to optimise is a key point. However, the definition of this cost function is not a trivial task. In the literature there are different articles in which the authors propose a particularized cost function depending on their preferences, as well as the application and architecture of the microgrid under study [21–23]. In many cases, their implementation requires the definition of weighting factors that lack physical meaning and are difficult to interpret and tune, even with a thorough knowledge of the microgrid [38]. Therefore, to improve its practical application in an MPC-based EMS it is relevant to have a cost function that combines the criteria of generality and extrapolability for its easy extension to other microgrids, interpretability by using physically meaningful parameters, and finally, standardisation, to avoid the use of weighting factors.

Table 3
Designer-defined costs for n ESS.

MEF_i	C_i^{var}	C_i^{fix}	C_i^{start}	C_i^{degr}
ch_1				
dis_1				
⋮				
ch_n				
dis_n				
$gridin$				
$gridout$				

Therefore, this section presents a methodology for the design of a generic MPC-based EMS, parameterizable, simple and with an easily interpretable cost function. It should be noted that this methodology can be extrapolated to other microgrid structures.

First, it is necessary to correctly define the PH. In a microgrid, especially with photovoltaic (PV) generation, there is usually a daily repetitive cyclic behaviour. For example, during the day there is a high solar resource, which usually leads to excess energy on the bus. However, in the afternoon/evening the solar resource is low or non-existent, which often results in an energy deficit situation. In addition, it is common that consumption patterns also follow daily patterns. For example, in a residential application, during the morning hours consumption is usually low because no one is at home, while in the afternoon and evening consumption increases considerably due to increased family activity. Therefore, to optimise this type of architecture and application of microgrids, it seems reasonable to define a PH = $24h$, as it allows to optimise a complete cycle. Of course, the PH can be adapted depending on the microgrid architecture or application under study.

Once the PH is defined, it is necessary to design the MPC. To carry out this design, the flowchart shown in Fig. 4 is defined. Thus, for each MEF_i, and considering both directions of energy flow, if applicable, the designer must define its costs (see Section 3.1), constraints and losses (see Section 3.2). Thus, the cost function J to be optimised is defined. Once all the MEFs are defined, it is necessary to define the boundaries of the microgrid state variables. Finally, the prediction profiles of the non-MEFs are defined.

3.1. Cost function

A generalised cost function to be optimised by the MPC is proposed where all the terms are associated to an economic cost (in this case in €), Eq. (9). In this way, the units of all the summands are equal, with physical sense, being more intuitive for the designer. This function uses the information for each sample time of the PH, as well as for each MEF of the microgrid.

$$J = \sum_{k=1}^{PH} \sum_{i=MEF}^{|MEF|} C_i^{var}(k) \cdot P_i(k) \cdot T_s + C_i^{fix}(k) \cdot WT_i(k) \cdot T_s + C_i^{start}(k) \cdot Start_i(k) + C_i^{degr}(k) \cdot \delta P_i^2(k) \tag{9}$$

Where C_i^{var}, C_i^{fix}, C_i^{start} and C_i^{degr} are user-defined costs, WT_i, $Start_i$ and

δP_i are decision variables and are defined in the following subsections.

The proposed approach aims to facilitate the definition of the MPC. All the MEFs involved in the microgrid can have the same type of costs (variable, fixed, start-up and degradation). Thus, for any microgrid architecture it is necessary to define for each MEF_i the following cost terms: variable cost C_i^{var}, fixed cost C_i^{fix}, start-up cost C_i^{start} and degradation cost C_i^{degr}.

Therefore, for a generic microgrid, the user should define the costs seen in Table 3. It should be noted that many of these costs may be zero. If the microgrid is modified, for example, by the appearance of a new ESS (supercapacitor, etc.) the index is maintained. In this case, it is only necessary to define the costs associated with the new MEF (new row for the charging and discharging process in Table 3).

3.1.1. Variable cost

A variable cost C_i^{var} in $€/Wh$ is defined, which determines the cost per Wh consumed, and by its definition, this cost is proportional to the operating power (P_i) of each MEF_i, see Eq. (9). Variable cost typically models those terms associated with the cost of energy, consumption of operating power-dependent supplies, the O&M cost per Wh, the depreciation cost per Wh or cost associated with CO_2 emissions.

Some general considerations for the definition of cost of energy depending on the microgrid architecture are the following: this term is associated with the cost of energy generated/consumed externally to the microgrid necessary to carry out the charging/discharging processes of the ESSs, or the purchase/sale of energy in the case of the MEG. In this sense, if it is considered that the energy used entirely for the charging/discharging processes of a certain ESS_j is contemplated in the power balance according to Eq. (5), or that the energy not contemplated is negligible, its operation does not derive costs of energy. A clear example occurs in microgrids that have HBBSs in which the cycle of production and storage of H_2 for subsequent use is carried out entirely from the surplus energy in the bus. Thus, $C_{ch_{H2}}^{var}$ and $C_{dis_{H2}}^{var}$ for HBBs can be zero (or negligible) [38–41]. Otherwise, these costs must be considered.

Finally, the use of MEG, when applicable, always has a variable cost due to the price of energy [36]. The purchase of energy from the grid has a cost in $€/Wh$, and logically, the higher the power consumed, the higher the term $C_i^{var} \cdot P_i$ in the cost function. These variable costs will always be positive in any MEF_i (economic cost), except in the sale of energy to the MEG where an economic benefit will be obtained. Therefore, $C_{var_{gridout}}$ is the only negative variable cost (although it is defined positive in Table 3, it must be negative in the equations).

In addition, C_i^{var} may include variable costs associated with the consumption of operating power-dependent supplies. An example of this is given in HBSSs where the cost of water and oxygen gas consumption by ELECs and FCs respectively can be considered.

Similarly, the variable cost may aggregate all those costs associated with O&M tasks required after a given MEF_i generates/consumes a given power. For example, BSSs may need to perform certain maintenance tasks after a certain number of charge or discharge cycles (i.e. a certain number of Wh) [38–41]. Thus, the O&M cost per Wh is calculated as the quotient between the cost and the number of Wh after which these tasks are performed. This is not the case for HBSSs for which the O&M costs per hour of operation are usually considered (as fixed costs, see Section 3.1.2). Similarly, the operation of the MEG does not derive O&M costs.

Analogously, C_i^{var} can include terms associated with depreciation cost. Thus, for example, battery lifetime is given by manufacturers as a number of charge/discharge cycles [42,43]. Thus, it is possible to calculate the battery cost per Wh extracted/stored in the BSSs (directly proportional to the number of cycles). The same applies to any other ESS.

Finally, in microgrid architectures where fossil fuel-based MEF_i exist, this cost can also model the cost associated with CO_2 emissions.

3.1.2. Fixed cost

The fixed cost C_i^{fix} in $€/h$ is the hourly operating cost for a given MEF_i, and by its definition, is independent of its operating power, see Eq. (9). To consider this cost, the binary variable working time WT_i of each MEF_i is defined. This decision variable indicates whether a given MEF_i produces/consumes energy, in short, whether it is operating. Thus, the product $C_i^{fix} \cdot WT_i$ produces an economic cost when the MEF_i produces/consumes energy ($WT_i = 1$). If the MEF does not produce/consume energy, this product will not produce any cost ($WT_i = 0$).

Fixed cost can be mainly due to two types of costs, fixed O&M and depreciation costs per operating h. Some general considerations for the definition of O&M costs depending on the microgrid architecture are the following: during the operation of BSSs and MEG, fixed O&M costs are not usually contemplated (or they are considered negligible) [39]. In contrast, these costs are usually considered in the operation of HBSSs [42,43]. Examples are the costs associated with detecting H2 leaks in tanks or pipelines during operation or checking cell voltages in FCs every few hours of operation. For this term, once the system is on, the power at which the system operates is indifferent.

Finally, C_i^{fix} can also contemplate the depreciation cost. For example, normally the HBSS has several operating hours with acceptable performance (e.g., with a degradation of $<20\%$) [42,43]. In this case, it is not relevant the power at which these systems work, but the operating hours. Thus, it is possible to calculate the depreciation cost as the quotient between acquisition cost and number of acceptable operating hours.

3.1.3. Start-up cost

A start-up cost C_i^{start} in $€/W^2$ is defined. This cost will only be considered at the instant when a given MEF_i goes from a non-operating condition (does not supply/consume energy) to supplying/consuming energy ($Start_i = 1$), in short, starts operating. In this case, the binary variable $Start_i(k)$ indicates whether a given MEF_i switches from not to provide/consume energy to produce/consume energy at instant k: $Start_i(k) = WT_i(k) \bigwedge \sim WT_i(k-1)$.

The start-up cost is usually related to the cost of starting up a system and the possible degradation costs resulting from this operation.

Some general considerations for the definition of start-up costs depending on the architecture of the microgrid are the following: during the operation of BSSs and MEG, start-up costs are not usually contemplated [39]. However, these costs are usually considered in the operation of HBSSs [9].

Similarly, C_i^{start} can also integrate certain degradation costs associated with the repetitive start-up and shut-down processes of MEFs. Perhaps the clearest example is the considerable degradation suffered in HBSSs (mainly in FCs) during start-up and shut-down processes due to various electrochemical phenomena [44,45]. Thus, it is possible to add in this cost a term related to this issue.

3.1.4. Degradation cost

A degradation cost C_i^{degr} in $€/W^2$ is defined. This cost penalises the degradation associated with variations in operating power for a given MEF_i of the microgrid, since these fluctuations can cause them to degrade greatly, e.g., in the case of HBSSs [9]. Then, C_i^{degr} is related to degradation cost due to power fluctuations.

Therefore, this term seeks to prevent these systems from operating with fluctuating power profiles, to favour smooth operation around their nominal or optimum operating power, at which they normally reach their highest efficiency. To this end, it is desirable to allow the system to reach this condition quickly. Based on the above, it is necessary not to penalise power variations during the start-up (minimum time needed for a system to reach its nominal/optimal power) and shut-down process (if desired). Thus, during the start-up process, it should be free to reach nominal power without penalising the cost function. Once the start-up

Table 4
Designer-defined constraints for n ESS.

MEF_i	$[\underline{P_i}, \overline{P_i}]$	$[\underline{\Delta P_i}, \overline{\Delta P_i}]$	$Loss_i$	$Loss_i^{BoP}$
ch_1				
dis_1				
⋮				
ch_n				
dis_n				
$gridin$				
$gridout$				
State Vector Constraints				
$\overline{SOC_1}$, $\underline{SOC_1}$, …, $\overline{SOC_n}$, $\underline{SOC_n}$, $\overline{V_{BUS}}$ (if applicable), $\underline{V_{BUS}}$ (if applicable)				
Initial conditions				
SOC_1^{ini}, …, SOC_n^{ini}, V_{BUS}^{ini} (if applicable)				

process is complete, the fluctuations in operating power can be penalised. For this reason, the power variation δP_i (see Eq. (10)) is defined as the variations in operating power ΔP_i at every sample time except during the start-up process.

$$\delta P_i = \Delta P_i \cdot Y_i.$$

Where:

$$Y_i = (WT_i(k) \wedge WT_i(k-1) \wedge \ldots \wedge WT_i(k-NTs_i)) \quad (10)$$

Where NTs_i is the number of sampling periods necessary for the MEF_i to reach nominal power (start-up process), and "∧" refers to the logical operation "*and*" between binary variables. The start-up process can last 1 or several sampling periods. For example, suppose the electrolyzer (MEF_{els}) has a start-up process of 3 sampling periods. In this scenario, $\delta P_{els} = \Delta P_{els} \cdot (WT_{els}(k) \bigwedge WT_{els}(k-1) \bigwedge WT_{els}(k-2) \bigwedge WT_{els}(k-3))$. Once the electrolyzer is turned on, in the following three samples, its variations will not be penalised ($\delta P_{els} = 0$ due to $WT_{els}(k-3) = 0$). At sampling k, the electrolyzer turns on, and, therefore, $WT_{els}(k) = 1$, $WT_{els}(k-1) = 0$, $WT_{els}(k-2) = 0$ and $WT_{els}(k-3) = 0$ ($\delta P_{els} = 0$ because $Y_{els} = 0$). At sampling $k+1$: $WT_{els}(k) = 1$, $WT_{els}(k-1) = 1$, $WT_{els}(k-2) = 0$ and $WT_{els}(k-3) = 0$ ($\delta P_i = 0$ because $Y_{els} = 0$). At sampling $k+2$: $WT_{els}(k) = 1$, $WT_{els}(k-1) = 1$, $WT_{els}(k-2) = 1$ and $WT_{els}(k-3) = 0$ ($\delta P_i = 0$ because $Y_{els} = 0$). Finally, at sampling $k+3$ (three sample times after power on): $WT_{els}(k) = 1$, $WT_{els}(k-1) = 1$, $WT_{els}(k-2) = 1$ and $WT_{els}(k-2) = 1$ ($Y_{els} = 1$). From this point on, power increases will be penalised: $\delta P_{els} = \Delta P_{els} \cdot Y_{els}$.

In this sense, it is necessary to consider that adding the cost term C_i^{degr} to MEFs with start-up processes of several sampling periods considerably increases the number of variables and constraints in the optimisation problem. In the proposed cost function, Eq. (9), δP_i is squared to penalise positive and negative increments indistinctly, and therefore, the consideration of C_i^{degr} leads to a quadratic optimisation problem (QP).

Finally, as for the previous cost terms, certain considerations can be established based on the MEFs commonly used in microgrids. For example, it is common to consider that during the operation of BSSs and MEG, degradation costs are not considered (or are considered negligible in the case of BSSs) [39]. In contrast, degradation costs can be considered in the operation of HBSSs [9].

3.2. Constraints

A microgrid must always satisfy the non-MEF- (e.g., P_{load}) from the power generated by the non-MEF+ (e.g., P_{ren}) and the power provided by the MEFs, in short, guarantee the power balance according to (5). To this end, in practice, there are physical and operational constraints that must be considered in the operation of any device. Therefore, once the control-oriented model and the cost function have been defined, it is necessary to define in general terms the constraints that will determine the operation of the microgrid. Based on the above, a set of physical and operational constraints will initially be established for the control variables.

The first constraints are usually associated with physical limits imposed by each MEF_i, such as a minimum or maximum power limit that they can never exceed ($\underline{P_i} \le P_i \le \overline{P_i}$). Similarly, some operating constraints can be defined to establish certain constraints on the operation of certain MEF_i. For example, it is possible to limit the power variation of a MEF_i ($\underline{\Delta P_i} \le \Delta P_i \le \overline{\Delta P_i}$). This restriction may not be related to a physical limit, but is advisable in some ESSs, where fluctuating power profiles may lead to excessive degradation.

Analogously, certain constraints must be established with the objective of establishing which operation process is carried out at each time instant k, in those ESS_j in which it is physically impossible (or not advisable) to carry out the charging and discharging process simultaneously (or the sale and purchase of energy to the MEG). Thus, the constraint $WT_{ch_j} + WT_{dis_j} \le 1$ (or $WT_{gridin} + WT_{gridout} \le 1$) is defined.

Finally, the constraints and initial conditions of the state variables ($[SOC_1 \ldots SOC_n\ V_{BUS}]$, V_{BUS} if it is desired to control it) of the microgrid will be established. These constraints can represent both the physical operational limits, as well as recommended operating margins to guarantee a safe and efficient operation of the ESSs.

Thus, in general, for the definition of the constraints to which the optimisation problem will be subject, the user will have to define all the physical and operational constraints according to the structure proposed in Table 4 (for each MEF_i, n ESS).

3.3. Optimisation problem

The model describes the dynamics with linear equations (for more detail, see Section 2.2.4). The state variables of the state-space model are $x(k) = [SOC_1(k), \ldots, SOC_n(k), V_{BUS}(k)]$. With all described above, the MPC-based EMS is defined as the optimisation problem defined in Eq. (11). In this problem, the decision variables $z = [P_i(k), WT_i(k), Start_i(k), \delta P_i(k)]$ are defined for each MEF_i of the microgrid. The model acts as a constraint in the control problem ($\underline{x} \le x(k) \le \overline{x}$ and $x(k+1) = A \cdot x(k) + B \cdot u(k) + d$, please see Eq. (11)). The MPC-based EMS strategy proposed is an economic minimisation. Therefore, the goal is to minimise the economic cost.

$$\min_z J(z)$$

Where:

$$J = \sum_{k=1}^{PH} \sum_{i=MEF}^{|MEF|} C_i^{var}(k) \cdot P_i(k) \cdot T_s + C_i^{fix}(k) \cdot WT_i(k) \cdot T_s + C_i^{start}(k) \cdot Start_i(k) + C_i^{degr}(k) \cdot \delta P_i^2(k)$$

Subject to:

$$\underline{P_i} \cdot WT_i(k) \le P_i(k) \le \overline{P_i} \cdot WT_i(k) \forall i \in MEF_i$$

$$\underline{\Delta P_i} \le \Delta P_i(k) \le \overline{\Delta P_i}\ \forall i \in MEF_i$$

$$WT_{ch_j}(k) + WT_{dis_j}(k) \le 1 \forall j \in ESS_j$$

$$WT_{gridin}(k) + WT_{gridout}(k) \le 1$$

$$\underline{x} \le x(k) \le \overline{x} \forall x(k)$$

$$x(k+1) = A \cdot x(k) + B \cdot u(k) + d$$

$$P_{nMEF+} - P_{nMEF-} - Loss(k) + P_{grid}(k) + \sum_{j=1}^{n} P_j(k) = 0 \quad (11)$$

The optimisation problem posed in (11) can be adapted to any type of microgrid architecture or application, and certain assumptions can be applied in its definition to significantly simplify its complexity:

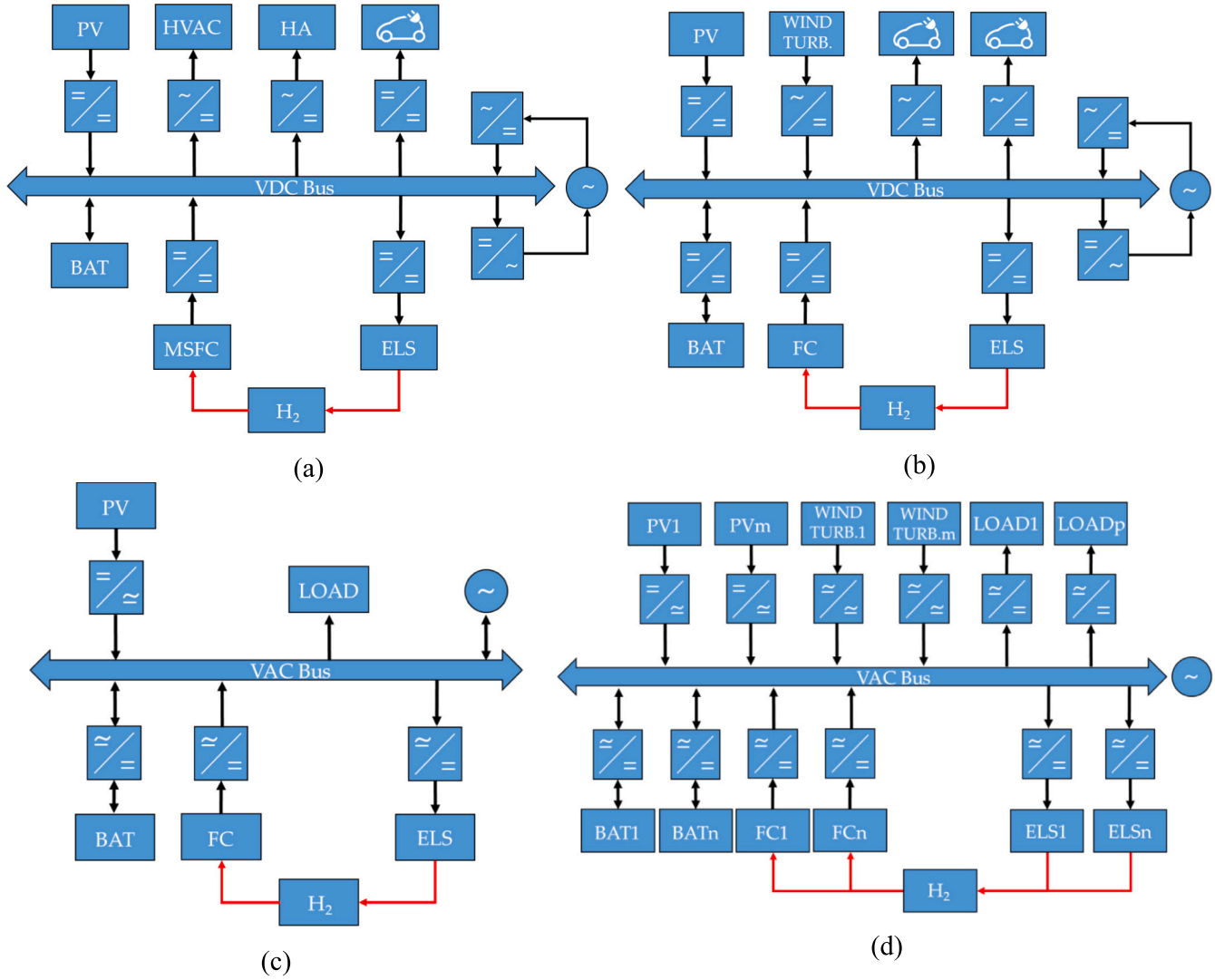

Fig. 5. Microgrid architecture for: (a) residential application (case 1); (b) electric vehicle charging station application (case 2); (c) industrial application (case 3); and (d) community application (case 4).

- Variable $WT_{dis_j}(k)$ or $WT_{ch_j}(k)$ can be eliminated for MEF_i that: 1) contain no fixed costs C_i^{fix}, 2) have no fixed losses due to BoP $Loss_i^{BoP}$.
- Variable $Start_i(k)$ can be removed in MEF_i that do not contemplate start-up costs C_i^{start}.
- Variable $\delta P_i(k)$ can be eliminated in MEF_i that do not contemplate degradation costs C_i^{degr}.

For example, the BSS usually does not contemplate fixed costs C_i^{fix} or losses due to BoP $Loss_i^{BoP}$. Therefore, it is possible to eliminate one of the two variables $WT_{dis_{bat}}(k)$ or $WT_{ch_{bat}}(k)$. For example, if the variable $WT_{dis_{bat}}$ is removed, this variable will be replaced by $(1 - WT_{ch_{bat}}(k))$ in the rest of the constraint. In this case, the constraint that does not allow the BSS to be used in charge and discharge mode simultaneously $(WT_{ch_{bat}}(k) + WT_{dis_{bat}}(k) \leq 1)$ should also be removed. Furthermore, the terms associated with $WT_{dis_{bat}}$ can be eliminated from the power balance, since there are no losses associated with the BoP. Similarly, this simplification can be performed in the grid (variable $WT_{gridin}(k)$ or $WT_{gridout}(k)$).

When a ESS_j (or MEG) has no start-up costs C_i^{start} the decision variable $Start_i(k)$ can be eliminated. In addition, when a ESS_j (or MEG) has no degradation costs C_i^{degr} the decision variable $\delta P_i(k)$ can be removed. The BSS and the MEG usually do not have these two costs.

Therefore, it can be eliminated the variables: $WT_{bat_{ch}}(k)$ or $WT_{bat_{dis}}(k)$, $WT_{gridin}(k)$ or $WT_{gridout}(k)$, $Start_{bat_{ch}}(k)$, $Start_{bat_{dis}}(k)$, $Start_{gridin}(k)$, $Start_{gridout}(k)$, $\delta P_{bat_{ch}}(k)$, $\delta P_{bat_{dis}}(k)$, $\delta P_{gridin}(k)$ y $\delta P_{gridout}(k)$.

Depending on the final formulation of the optimisation problem, according to (11), a MILP (linear cost function) or MIQP (quadratic cost function) will be used to solve it, depending on whether the cost function integrates the degradation cost term (C_i^{degr}) for any MEF_i.

4. Case studies: results & discussion

This section validates the proposed MPC-based EMS modelling and design methodology on different microgrid architectures and applications. With this goal in mind, multiple simulations have been performed in MATLAB Simulink® with the YALMIP toolbox and IBM CPLEX Optimiser solver for MILP and MIQP optimisation problems.

In this study, four microgrid architectures specially designed to provide solutions for different applications are distinguished: residential application, EVs charging station, industrial application and community application. Each architecture differs in scale, bus architecture, microgrid configuration and constraints. These cases will be detailed below.

For all cases it has been assumed that non-MEF+ are associated with renewable energy sources ($P_{nMEF+} = P_{ren}$), mainly photovoltaic and

Table 5
Design parameters, costs, constraints and losses defined for case 1.

Case	ESS parameters								
	CN_{bat} = 28.8 kWh		η_{ch}^{bat} = 0.934	η_{dis}^{bat} = 1	CN_{H2} = 24 kWh		η_{ch}^{H2} = 0.57		η_{dis}^{H2} = 0.57
	$K_{V_{BUS}}$ = 0.01		K_{SOC} = 30		K_{Pch} = 0.002		K_{Pdis} = 0.002		v_k = 355
	MPC Parameters & Constraints								
	MEF_i	C_i^{var}	C_i^{fix}	C_i^{start}	C_i^{degr}	$[\underline{P_i}, \overline{P_i}]$	$[\underline{\Delta P_i}, \overline{\Delta P_i}]$	$Loss_i$	$Loss_i^{BoP}$
	ch_{bat}	0.4 €/MWh	–	–	–	[0,10] kW	–	–	–
	dis_{bat}	0.4 €/MWh	–	–	–	[0, 6] kW	–	–	–
	ch_{H2}	–	0.015 €/h	0.05 €	0.05 €/W^2	[0, 5] kW	–	0.05	1 kW
1	dis_{H2}	–	0.028 €/h	0.05 €	0.05 €/W^2	[0, 3.5] kW	–	0.05	300 W
	gridin	Table 10	–	–	–	[0, 6] kW	–	0.05	–
	gridout	0.05 €/MWh	–	–	–	[0, 10] kW	–	0.05	–
	State Vector Constraints								
	$\overline{SOC_{bat}}$ = 90%, $\underline{SOC_{bat}}$ = 55%, $\overline{SOC_{H2}}$ = 100%, $\underline{SOC_{H2}}$ = 25%, $\overline{V_{BUS}}$ = 450 V, $\underline{V_{BUS}}$ = 330 V								
	Initial conditions								
	V_{BUS}^{ini} = 375 V, SOC_{bat}^{ini} = 56%, SOC_{H2}^{ini} = 25%								

wind energy. The prediction of renewable generation has been developed from real measurements of solar radiation and wind speed for the province of Huelva, Spain. Likewise, the non-MEF- are defined by the different loads associated with each microgrid architecture and application ($P_{nMEF-} = P_{load}$). These profiles are based on real applications or typical consumptions provided by the Institute for the Diversification and Saving of Energy (IDAE) [46] and the Spanish national electricity system operator (REE) [47].

To define the model and the controller for each of the cases under study, the proposed methodology has been used, specifically the flow diagrams defined in Figs. 3 and 4, as well as the Tables 2-4. The characteristic parameters in terms of performance and costs associated with ESSs and MEG have been obtained from average values of commercial equipment datasheets and cost terms presented in the scientific literature for similar applications and microgrids, respectively. Depreciation costs have not been considered in any architecture due to two reasons: 1) not to limit the use of available devices due to their acquisition cost and 2) it is possible to analyse the profitability of the system offline. We think that economic depreciation should not be considered in daily operations. When a device is purchased, the objective is to obtain the highest economic performance and not to limit its use due to the acquisition cost. Costs related to degradation effects are already considered in the cost function.

For simulations, in all scenarios a prediction horizon (PH) of 24h has been considered (a daily repetitive cyclic behaviour is assumed) and a sampling time (T_s) of 0.033 h (120 s.). Each case has been simulated in different scenarios, considering different initial conditions, starting time, weather conditions (sunny, cloudy, sunless, windy, windless, etc.), etc. Finally, in order to avoid that the ESSs end up with SOCs close to the minimum levels established, constraints have been included in which their SOCs must be greater than or equal to the initial one ($SOC_{bat}^{end} \geq SOC_{bat}^{ini}$ y $SOC_{H2}^{end} \geq SOC_{H2}^{ini}$). By doing so, all simulations start and end with approximately the same level of SOCs, making it fairer to compare the economic cost obtained by the EMS (no energy is used from previous operations).

4.1. Case studies

4.1.1. Case 1: residential application

In this case, a microgrid architecture adapted to a grid-connected residential application is proposed, Fig. 5a. As renewable generation sources, a PV field is used ($P_{ren} = P_{PV}$), while the loads are determined by the house appliances (P_{HA}), the consumption of the ventilation and air conditioning system (P_{HVAC}) and the charge process of an electric vehicle (P_{EV}), $P_{load} = P_{HVAC} + P_{HA} + P_{EV}$. A HESS composed of a BSS, which supports the DC bus, and a HBSS is also available. In this case, a first-order Thevenin equivalent model has been considered for BSS modelling and hence the DC bus voltage [48]. The sizing parameters of the microgrid are shown in Table 5.

For the definition of the MPC, it will be necessary to define the constraints, losses and cost terms of each of the MEFs that determine the microgrid architecture according to the proposed methodology.

Thus, according to the provisions of Section 3, for the BSS only a variable O&M cost will be considered (in the literature these costs are defined between [0.3–0.5] €/MWh [49–51]). Likewise, due to the direct connection to the DC bus, no losses related to its use (nor BoP) will be considered.

Regarding the HBSS, no variable costs will be considered since device consumptions are already implicitly considered in the energy balance. On the contrary, for HBSS it is necessary to define fixed costs (due

Table 6
Design parameters, costs, constraints and losses defined for case 2.

Case	ESS parameters								
	CN_{bat} = 32.4 kWh		η_{ch}^{bat} = 0.9	η_{dis}^{bat} = 1	CN_{H2} = 24 kWh		η_{ch}^{H2} = 0.57		η_{dis}^{H2} = 0.57
	MPC Parameters & Constraints								
	MEF_i	C_i^{var}	C_i^{fix}	C_i^{start}	C_i^{degr}	$[\underline{P_i}, \overline{P_i}]$	$[\underline{\Delta P_i}, \overline{\Delta P_i}]$	$Loss_i$	$Loss_i^{BoP}$
	ch_{bat}	0.4 €/MWh	–	–	–	[0,20] kW	–	0.05	–
	dis_{bat}	0.4 €/MWh	–	–	–	[0, 10] kW	–	0.05	–
	ch_{H2}	–	0.015 €/h	0.05 €	–	[0, 10] kW	[−2,2] kW/T_s	0.05	3.5 kW
2	dis_{H2}	–	0.028 €/h	0.05 €	–	[0, 5] kW	[−2, 2] kW/T_s	0.05	750 W
	gridin	Table 10	–	–	–	[0, 10] kW	–	0.05	–
	gridout	0.05 €/MWh	–	–	–	[0, 20] kW	–	0.05	–
	State Vector Constraints								
	$\overline{SOC_{bat}}$ = 90%, $\underline{SOC_{bat}}$ = 55%, $\overline{SOC_{H2}}$ = 100%, $\underline{SOC_{H2}}$ = 14%								
	Initial conditions								
	SOC_{bat}^{ini} = 90%, SOC_{H2}^{ini} = 100%								

Table 7
Design parameters, costs, constraints and losses defined for case 3.

Case	ESS parameters								
	$CN_{bat} = 252$ kWh		$\eta_{ch}^{bat} = 0.934$		$\eta_{dis}^{bat} = 1$	$CN_{H2} = 240$ kWh	$\eta_{ch}^{H2} = 0.57$		$\eta_{dis}^{H2} = 0.57$
	MPC Parameters & Constraints								
	MEF_i	C_i^{var}	C_i^{fix}	C_i^{start}	C_i^{degr}	$[\underline{P_i}, \overline{P_i}]$	$[\underline{\Delta P_i}, \overline{\Delta P_i}]$	$Loss_i$	$Loss_i^{BoP}$
	ch_{bat}	0.4 €/MWh	–	–	–	[0, 150] kW	–	0.05	–
	dis_{bat}	0.4 €/MWh	–	–	–	[0, 50] kW	–	0.05	–
	ch_{H2}	–	0.015 €/h	0.01 €	–	[0, 60] kW	$[-4, 4]$ kW/T_s	0.05	10 kW
3	dis_{H2}	–	0.028 €/h	0.01 €	–	[0,30] kW	$[-4, 4]$ kW/T_s	0.05	3.5 kW
	gridin	Table 10	–	–	–	[0, 50] kW	–	–	–
	gridout	0.06 €/MWh	–	–	–	[0, 150] kW	–	–	–
	State Vector Constraints								
	$\overline{SOC_{bat}} = 90\%$, $\underline{SOC_{bat}} = 55\%$, $\overline{SOC_{H2}} = 100\%$, $\underline{SOC_{H2}} = 10\%$								
	Initial conditions								
	$SOC_{bat}^{ini} = 75\%$, $SOC_{H2}^{ini} = 58\%$								

to O&M costs, defined in the literature between [0.001–0.1] €/*h* [9,52–54], start-up costs (defined in the literature between [0.01–0.123] € [9,55]) and degradation costs (defined in the literature between [0.01–0.05] €/W^2 [9,55]). These values will be used as reference for all cases. In addition, variable losses, due to the power converters and related to their BoPs, are defined.

Finally, considering the MEG, a variable energy purchase cost will be considered (see Table 10), while the energy sale cost is considered fixed. In contrast, the MEG has no fixed, start-up or degradation costs. Moreover, the connection of the MEG to the DC bus entails variable losses associated with the power converters.

Considering the constraints, in addition to the usual ones, associated to the physical limits of operation of the devices, as well as the manufacturer's recommendations, it is necessary to establish constraints associated to the state vector. In addition, it is necessary to establish constraints for the definition of the decision variables $Start_i$ (see Section 3.1.3) and δP_i (see Section 3.1.4). These constraints are defined by conversion of logic relations into mixed-integer inequalities [56,57]. In this case, no constraints have been considered for the variation of the power. Thus, in this case, an MIQP with 27,360 inequality and 720 equality constraints is used.

According to the designed methodology, the state space model of the microgrid, decision variables, cost function and constraints of the optimisation problem under study are defined in Tables 5 and 9.

4.1.2. Case 2: electric vehicles charging station

In this case, a microgrid architecture adapted to a grid-connected electric vehicle (EV) charging station is proposed, Fig. 5b. A photovoltaic field (P_{PV}) and a wind generator (P_W) are used as renewable energy sources ($P_{ren} = P_{PV} + P_W$), while the loads are determined by the consumption associated to two EV charging points (P_{EV_1}, P_{EV_2}), assumed operating at constant charging power $P_{load} = P_{EV1} + P_{EV2}$. A HESS consisting of a BSS, and a HBSS is also available. The BSS is not directly connected to the DC bus. The sizing parameters of the microgrid are shown in Table 6. As in the previous case, for the definition of the MPC, it will be necessary to define the constraints, losses and cost terms of each of the MEFs that determine the architecture of the microgrid according to the proposed methodology.

Thus, in accordance with the provisions of Section 3, and analogously to the previous case, the costs terms are defined. Unlike the previous case, in this case losses in the BSS due to the power converter will be considered. In this case, no degradation costs are contemplated for the HBSS. Regarding the constraints, parameters very similar to those of the previous case will be defined, with the exception that according to the microgrid architecture, it is not necessary to establish the constraint related to the DC bus voltage. Likewise, restrictions on the variation of the HBSS operating power and variable losses in the BSS due to the connection through the converter to the bus have been considered. In this case, a MILP with 18,720 inequalities and 720 equality constraints is used. According to the designed methodology, Tables 6 and 9 define the state space model of the microgrid, the decision variables, the cost function and the constraints of the optimisation problem under study.

4.1.3. Case 3: industrial application

In this case, a microgrid architecture adapted to an industrial application connected to the grid over an AC bus is proposed, Fig. 5c. A photovoltaic field (P_{PV}) installed on the roof of the industry is used as a renewable energy source ($P_{ren} = P_W$), while the load is determined by the consumption associated with the industrial consumption, characterised as a stable consumption profile (P_{load}). As in the previous cases, a HESS composed of an BSS and a HBSS is available. In accordance with

Table 8
Design parameters, costs, constraints and losses defined for case 4.

Case	ESS parameters								
	$CN_{bat} = 135$ kWh		$\eta_{ch}^{bat} = 0.934$		$\eta_{dis}^{bat} = 1$	$CN_{H2} = 120$ kWh	$\eta_{ch}^{H2} = 0.57$		$\eta_{dis}^{H2} = 0.57$
	MPC Parameters & Constraints								
	MEF_i	C_i^{var}	C_i^{fix}	C_i^{start}	C_i^{degr}	$[\underline{P_i}, \overline{P_i}]$	$[\underline{\Delta P_i}, \overline{\Delta P_i}]$	$Loss_i$	$Loss_i^{BoP}$
	ch_{bat}	0.4 €/MWh	–	–	–	[0,100] kW	–	0.05	–
	dis_{bat}	0.4 €/MWh	–	–	–	[0, 50] kW	–	0.05	–
	ch_{H2}	–	0.015 €/h	0.01 €	–	[5] kW	–	0.05	1 kW
4	dis_{H2}	–	0.028 €/h	0.01 €	–	[3.5, 3.5] kW	–	0.05	300 W
	gridin	Table 10	–	–	–	[0, 50] kW	–	–	–
	gridout	0.05 €/MWh	–	–	–	[0, 100] kW	–	–	–
	State Vector Constraints								
	$\overline{SOC_{bat}} = 90\%$, $\underline{SOC_{bat}} = 55\%$, $\overline{SOC_{H2}} = 100\%$, $\underline{SOC_{H2}} = 11\%$								
	Initial conditions								
	$SOC_{bat}^{ini} = 75\%$, $SOC_{H2}^{ini} = 55\%$								

Table 9
Necessary parameters for the definition of the microgrid model for n ESSs and DC bus supported by ESS.

Cases	Model
1	$\begin{bmatrix} SOC_{bat}(k+1) \\ SOC_{H2}(k+1) \\ V_{BUS}(k+1) \end{bmatrix} = \begin{bmatrix} 1 & 0 & 0 \\ 0 & 1 & 0 \\ K_{SOC} & 0 & K_{V_{BUS}} \end{bmatrix} \begin{bmatrix} SOC_{bat}(k) \\ SOC_{H2}(k) \\ V_{BUS}(k) \end{bmatrix} + \begin{bmatrix} r_{ch}^{bat} & -r_{dis}^{bat} & 0 & 0 \\ 0 & 0 & r_{ch}^{H2} & -r_{dis}^{H2} \\ K_{P\,ch} & -K_{P\,dis} & 0 & 0 \end{bmatrix} \begin{bmatrix} P_{ch_{bat}}(k) \\ P_{dis_{bat}}(k) \\ P_{ch_{H2}}(k) \\ P_{dis_{H2}}(k) \end{bmatrix}$
2–4	$\begin{bmatrix} SOC_{bat}(k+1) \\ SOC_{H2}(k+1) \end{bmatrix} = \begin{bmatrix} 1 & 0 \\ 0 & 1 \end{bmatrix} \begin{bmatrix} SOC_{bat}(k) \\ SOC_{H2}(k) \end{bmatrix} + \begin{bmatrix} r_{ch}^{bat} & -r_{dis}^{bat} & 0 & 0 \\ 0 & 0 & r_{ch}^{H2} & -r_{dis}^{H2} \end{bmatrix} \begin{bmatrix} P_{ch_{bat}}(k) \\ P_{dis_{bat}}(k) \\ P_{ch_{H2}}(k) \\ P_{dis_{H2}}(k) \end{bmatrix}$
	Cost function
1	$minJ = \sum_{k=1}^{PH} \sum_{i=MEF}^{\lvert MEF \rvert} C_i^{var}(k) \cdot P_i(k) \cdot T_s + C_i^{fix}(k) \cdot WT_i(k) \cdot T_s + C_i^{start}(k) \cdot Start_i(k) + C_i^{degr}(k) \cdot \delta P_i^2(k)$
2–4	$minJ = \sum_{k=1}^{PH} \sum_{i=MEF}^{\lvert MEF \rvert} C_i^{var}(k) \cdot P_i(k) \cdot T_s + C_i^{fix}(k) \cdot WT_i(k) \cdot T_s + C_i^{start}(k) \cdot Start_i(k)$
	Decision variables
1	$P_{ch_{bat}}(k), P_{dis_{bat}}(k), P_{ch_{H2}}(k), P_{dis_{H2}}(k), P_{gridin}(k), P_{gridout}(k), WT_{ch_{bat}}(k), WT_{ch_{H2}}(k), WT_{dis_{H2}}(k), WT_{gridin}(k), Start_{ch_{H2}}(k), Start_{dis_{H2}}(k), \delta P_{ch_{H2}}(k), \delta P_{dis_{H2}}(k)$
2–4	$P_{ch_{bat}}(k), P_{dis_{bat}}(k), P_{ch_{H2}}(k), P_{dis_{H2}}(k), P_{gridin}(k), P_{gridout}(k), WT_{ch_{bat}}(k), WT_{ch_{H2}}(k), WT_{dis_{H2}}(k), WT_{gridin}(k), Start_{ch_{H2}}(k), Start_{dis_{H2}}(k)$
	Constraints
All cases	$\underline{P_{ch_{bat}}} \cdot WT_{ch_{bat}}(k) \le P_{ch_{bat}}(k) \le \overline{P_{ch_{bat}}} \cdot WT_{ch_{bat}}(k)$
	$\underline{P_{dis_{bat}}} \cdot (1 - WT_{ch_{bat}}(k)) \le P_{dis_{bat}}(k) \le \overline{P_{dis_{bat}}} \cdot (1 - WT_{ch_{bat}}(k))$
	$\underline{P_{ch_{H2}}} \cdot WT_{ch_{H2}}(k) \le P_{ch_{H2}}(k) \le \overline{P_{ch_{H2}}} \cdot WT_{ch_{H2}}(k)$
	$\underline{P_{dis_{H2}}} \cdot WT_{dis_{H2}}(k) \le P_{dis_{H2}}(k) \le \overline{P_{dis_{H2}}} \cdot WT_{dis_{H2}}(k)$
	$\underline{P_{gridin}} \cdot WT_{gridin}(k) \le P_{gridin}(k) \le \overline{P_{gridin}} \cdot WT_{gridin}(k)$
	$\underline{P_{gridout}} \cdot (1 - WT_{gridin}(k)) \le P_{gridout}(k) \le \overline{P_{gridout}} \cdot (1 - WT_{gridin}(k))$
	$\underline{SOC_{bat}} \le SOC_{bat}(k) \le \overline{SOC_{bat}}; \underline{SOC_{H2}} \le SOC_{H2}(k) \le \overline{SOC_{H2}}$
	$\underline{\Delta P_{els}} \le \Delta P_{els}(k) \le \overline{\Delta P_{els}}; \underline{\Delta P_{fc}} \le \Delta P_{fc}(k) \le \overline{\Delta P_{fc}}$
	$Start_i(k) = WT_i(k) \wedge \sim WT_i(k-1)$
	$\underline{V_{BUS}} \le V_{BUS}(k) \le \overline{V_{BUS}}$
1	$\delta P_i(k) = \Delta P_i(k) \wedge Y_i(k)$, with $Y_i(k) = WT_i(k) \wedge WT_i(k-1)$
4	$0 \le WT_{ch_{H_2}} \le N_{els}; 0 \le WT_{dis_{H2}} \le N_{fc}$
All cases	$P_{dis_{bat}}(k)(1 + Loss_{dis_{bat}}) - P_{ch_{bat}}(k)(1 + Loss_{ch_{bat}}) + P_{dis_{H2}}(k)(1 + Loss_{dis_{H2}}) + WT_{dis_{H2}}(k) \cdot Loss_{dis_{H2}}^{BoP} - P_{ch_{H2}}(k)(1 + Loss_{ch_{H2}}) + WT_{ch_{H2}}(k) \cdot Loss_{ch_{H2}}^{BoP} + P_{gridin}(k)(1 + Loss_{gridin}) - P_{gridout}(k)(1 + Loss_{gridout}) + P_{ren}(k) - P_{load}(k) = 0$

the Section 3, and analogously to the previous cases, the sizing parameters of the microgrid are shown in Table 7. In this case, variable losses in the grid have not been considered due to the direct connection to the AC bus. Thus, in this example, a MILP with 18,720 inequations and 720 equality constraints is used. According to the methodology designed, Table 7 and 9 define the state space model of the microgrid, the decision variables, the cost function and the constraints of the optimisation problem under study.

4.1.4. Case 4: community application

In the latter case, the microgrid architecture models a community application with multiple energy consumers and producers (prosumers) and is shown in Fig. 5d. In this example, a community with ten neighbours ($N_{br} = 10$) is defined. MEG connection is available to guarantee, at all times, the energy balance in the microgrid. Considering the community system as a whole, the complex system can be modelled by considering a single battery with the resulting capacity and voltage. For its application in a real system, a low-level control would be necessary to charge and discharge the batteries properly.

To elaborate on the above, on the one hand, the microgrid must satisfy the P_{load} of each neighbour in the community. On the other hand, the microgrid has renewable power P_{ren} generated by each neighbour. Thus, it is possible to consider: (1) the P_{load} of the community as the sum of the load powers of each neighbour $P_{load\,m}$ ($P_{load} = \sum_{m=1}^{\lvert N_{br} \rvert} P_{load\,m}$) and (2)

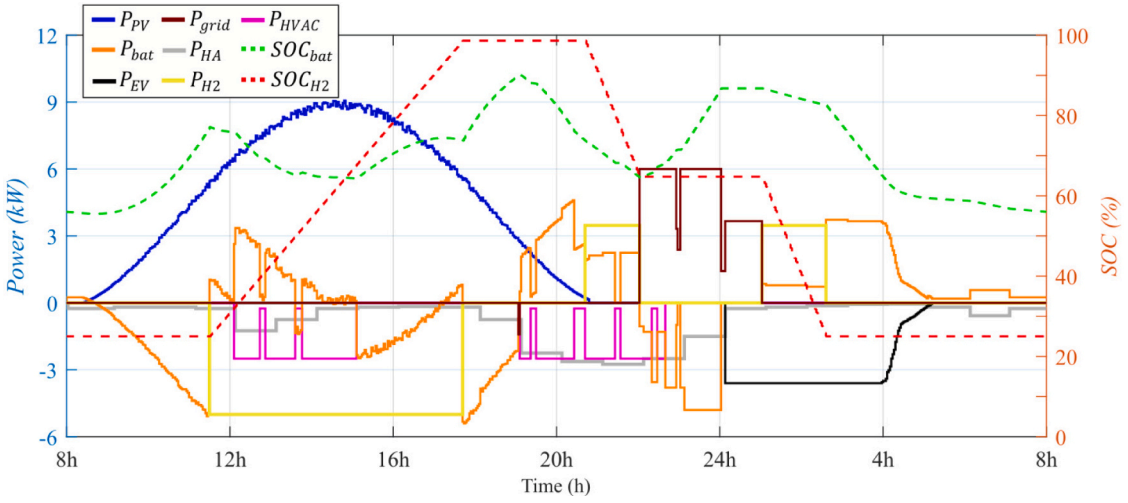

Fig. 6. Power and SOC profiles obtained for case 1 for a daily simulation.

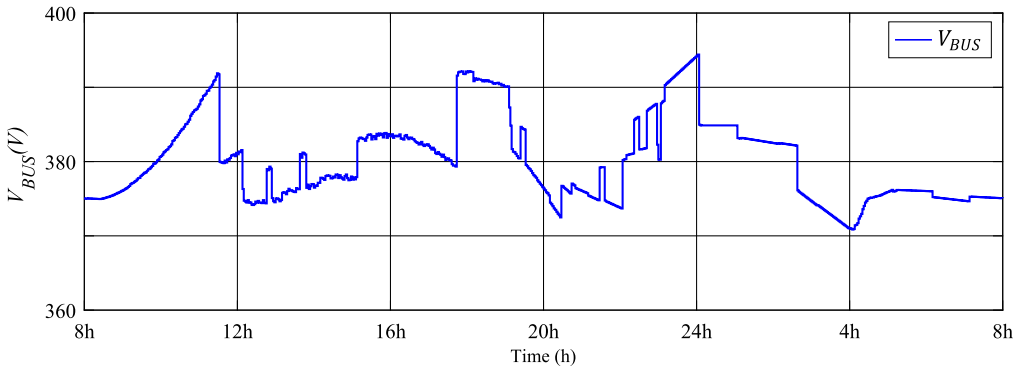

Fig. 7. DC bus voltage profile obtained for case 1 for a daily simulation.

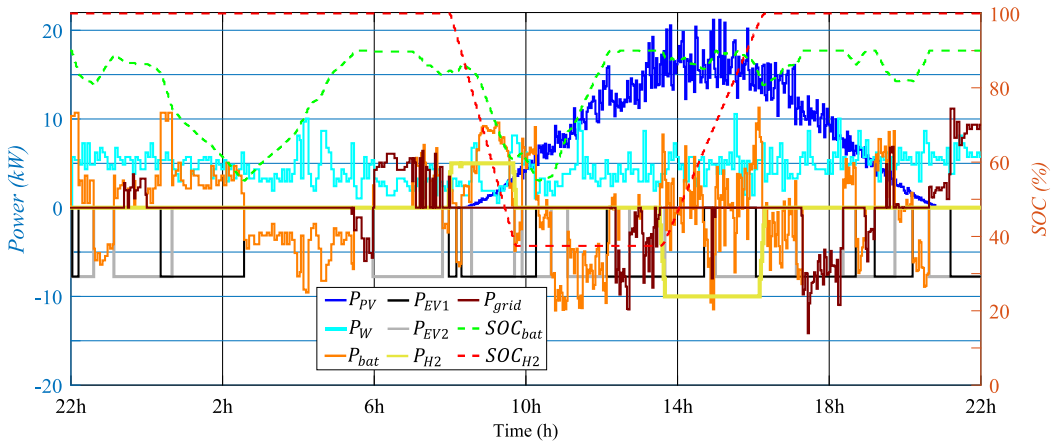

Fig. 8. Power and SOC profiles obtained for case 2 for a daily simulation.

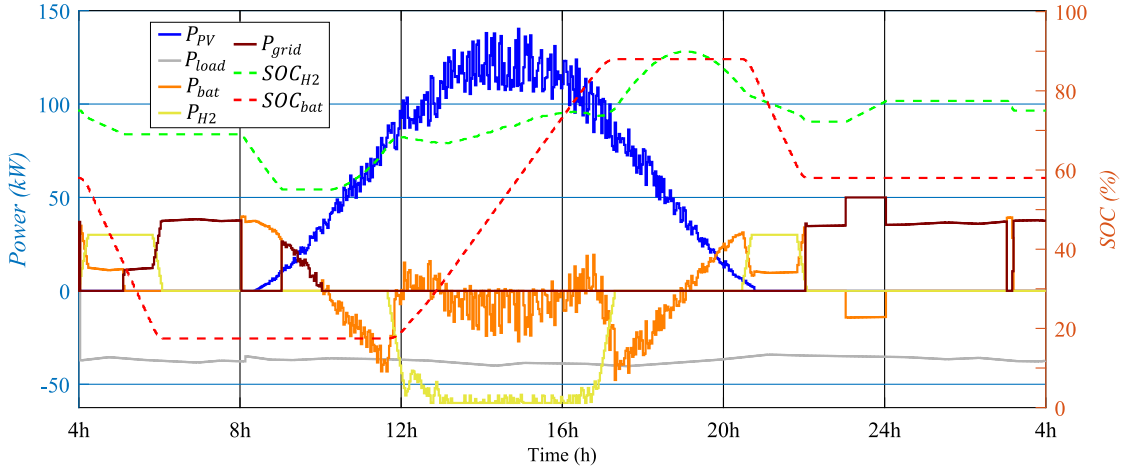

Fig. 9. Power and SOC profiles obtained for case 3 for a daily simulation.

the P_{ren} generated by the community as the sum of the power generated by each neighbour P_{PVm} ($P_{ren} = \sum_{m=1}^{|N_{br}|} P_{PVm}$). Of course, not all loads and renewable power act at the same time. In addition, each neighbour may have a different load and renewable power.

Under this concept, it will be considered that there is only one hydrogen tank in the community. Each neighbour may or may not have an ELEC and/or FC. In this example, it has been considered that the microgrid has six neighbours with ELEC (N_{els}= 6) and FC (N_{fc} = 6). To facilitate the study, in this case, each individual HBSS can only operate at rated power. Despite this assumption, the considerable number of devices available allows the required power generation/consumption profile to be adapted with great flexibility by switching one or more ELECs/FCs on or off.

To simulate this operation, the variables WT_i and $Start_i$, for the ELEC and FC, will now be integer variables in this example (unlike previous architectures, where they were binary because there was only one FC and ELEC). Thus, these variables will indicate the number of FCs or ELECs ON. Thus, for example, assuming that at sampling $k-1$, there are two ELECs previously connected ($WT_{els}(k-1) = 2$ and $Start_{els}(k-1) = 0$), and at sampling k, three more ELECs are connected ($WT_{els}(k) = 5$

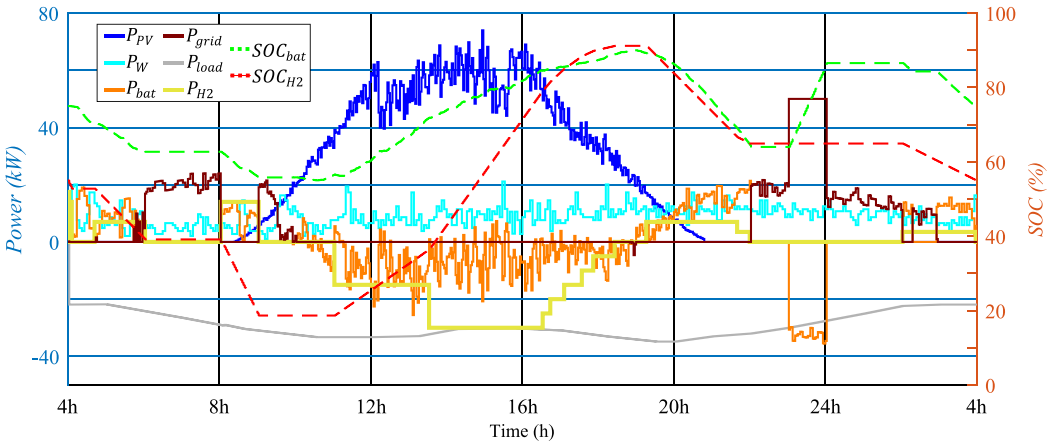

Fig. 10. Power and SOC profiles obtained for case 4 for a daily simulation.

and $Start_{els}(k) = 3$), which remain connected at instant $k+1$ ($WT_{els}(k+1) = 5$ and $Start_{els}(k+1) = 0$). So, at sampling $k-1$, $P_{ch_{H2}}$ will be two times the nominal power (3.5 kW) of the ELEC ($P_{ch_{H2}} = 2{\cdot}3.5$ kW). However, at sampling k, when connecting three more ELECs (five in all), $P_{ch_{H2}} = 5{\cdot}3.5$ kW. Finally, at sampling $k+1$ and so on, $P_{ch_{H2}} = 5{\cdot}3.5$ kW.

In accordance with Section 3, and analogously to the previous cases, the sizing parameters of the microgrid are shown in Table 8. For the ELEC ($i = els$) and FC ($i = fc$), the fixed cost (C_i^{fix}), start-up cost (C_i^{start}), and BoP will be defined by an individual system. Therefore, the term "$C_i^{fix}(k){\cdot}WT_i(k)$" of the cost index (see Eq. (9)) calculates the total fixed cost, considering all the ELECs or FCs operating at sampling k ($WT_i(k)$). In the same way, the term "$C_i^{start}(k){\cdot}Start_i(k)$" of the cost index (see Eq. (10)) calculates the total start-up cost, considering all the systems that have been turned on at sampling k. Again, the term "$Loss_i^{BoP}(k){\cdot}WT_i(k)$" of the balance equation (see Eq. (6)) calculates the total BoP loss, considering all systems that operate at sampling k ($WT_i(k)$).

Thus, in this example, a MILP with 19,440 inequations and 720 equality constraints is used. According to the methodology designed, Table 8 and 9 define the state space model of the microgrid, the decision variables, the cost function and the constraints of the optimisation problem under study.

4.2. Results

Regarding validation, almost 200 simulations (available in http://hdl.handle.net/10251/193290) have been carried out in this work for the four cases under study, for different initial conditions, ESS constraints, renewable resource profiles, etc. Due to lack of space, only some results of special interest are shown in this work.

The simulation results for the four cases under study are shown in Figs. 6-10. In all simulations, sunny and cloudy days have been considered. In the simulations, the powers injected into the DC bus are positively represented, while all power extracted from the DC bus has a negative sign. In particular, Fig. 6 shows the evolution of the microgrid power variables for case 1, as well as the SOCs of the BSS and HBSS for a radiation profile corresponding to that of a sunny day, and a typical residential consumption profile determined by three daily consumption peaks, during the early morning, midday and evening hours (see Fig. 6). Considering the integration method of the BSS in the DC bus, Fig. 7 shows the bus voltage evolution during the 24 h of simulation time.

Fig. 8 shows the evolution of the power variables and the SOC of the HESS for case 2, for a radiation profile corresponding to that of a sunny day with cloudy intervals with a high wind resource profile (see Fig. 8). On the other hand, the consumption profile associated with the EVs is defined by the nominal power of the charging points, assuming continuous operation from early morning (see Fig. 8).

Next, Fig. 9 shows the evolution of the power of MEF_i and SOC variables for the case 3 microgrid. In this case, a radiation profile of a sunny day with cloudy intervals has been considered. The power profile has been considered practically constant according to the profiles of industries operating 24 h a day (see Fig. 9).

Fig. 10 shows the evolution of the MEG and HESS power and SOC variables for the community system, case 4. For the simulation, a radiation profile corresponding to a cloudy day and a low wind generation profile has been considered. In this case, the consumption profile used corresponds to the scaled average annual demand profile for the city of Huelva (southwestern Spain).

Finally, Table 11 shows the economic cost for each of the cases, considering the proposed microgrid and MPC architecture ($Cost_{MPC}$), the case in which the microgrid has not ESS but a renewable generation ($Cost_{ren}$), and the traditional case based on the exclusive connection to the MEG ($Cost_{MEG}$).

4.3. Discussion

Although each case presents a different microgrid architecture and application, in general terms, the response of the MPC-based EMS designed for each case study generates common patterns in the use of HESS and MEG, and in short, the behaviour of the different microgrids is very similar. For this reason, a common discussion of the results can be carried out.

Regarding the use of the BSS, regardless of the method of integration to the DC bus, its operation is associated with its role as a fast response ESS with low operation cost, see Tables 5-8. This implies that the MPC promotes a more exhaustive use of the BSS to the benefit of a more conservative use of the HBSS, see Figs. 6, 8-10.

Thus, it is the BSS that acts in the first instance to guarantee the power balance on the bus, absorbing all fluctuations in the generation and demand profile, even during the start-up, shutdown and operation processes of the HBSS as can be seen in all simulations. Sometimes this occurs even when MEG operates (case 1: during the interval 22 h $\leq t \leq$ 23 h, Fig. 6 and case 4: interval 23 h $\leq t \leq$ 24 h, Fig. 10).

The operation of the BSS is mainly defined by the SOC_{bat} constraints, its lower and upper boundary values ($\underline{SOC_{bat}}$ and $\overline{SOC_{bat}}$), and the final constraint ($SOC_{bat}^{end} \geq SOC_{bat}^{ini}$). In the specific case 1, due to the DC bus integration method, its operation will also be determined by the DC bus voltage V_{BUS} constraints, see Fig. 6 and 7. It is verified that SOC_{bat} (all cases), and V_{BUS} (only for case 1) evolve and comply with the limits imposed by the constraints, see Figs. 6-10.

Considering the use of the HBSS, its operation is associated with its role as a slow response ESS, and that is why the MPC, in terms of cost, favours a more conservative use with respect to BSS, thus minimising the

Table 10
MEG hourly power purchase price between 22 h on 09/21/2022 and 22 h on 09/22/2022 in Spain.

Time (h)	Price (€/MWh)	Time (h)	Price (€/MWh)	Time (h)	Price (€/MWh)	Time (h)	Price (€/MWh)
22–23	336.62	04–05	392.72	10–11	391.41	16–17	298.46
23–00	318.02	05–06	389.31	11–12	377.38	17–18	324.77
00–01	357.04	06–07	364.61	12–13	373.21	18–19	386.86
01–02	377.73	07–08	375.18	13–14	368.95	19–20	417.00
02–03	384.00	08–09	426.10	14–15	307.02	20–21	498.26
03–04	388.94	09–10	380.72	15–16	296.07	21–22	485.62

Table 11
Hourly cost of operation for the four cases under study, for the microgrid and use of the MPC, architecture without ESS and traditional case of connection exclusively to the MEG.

Case	$Cost_{MPC}$ (€)	$Cost_{MPC}/Cost_{MEG}$(%)	$Cost_{rem}$ (€)	$Cost_{ren}/Cost_{MEG}$ (%)	$Cost_{MEG}$ (€)
1	5.40	30.56	10.40	58.86	17.67
2	6.87	10.11	15.96	23.48	67.97
3	122.36	36.71	162.88	48.86	333.34
4	54.83	21.75	82.73	32.82	252.06

number of operating cycles, to reduce the associated cost.

Regardless of the case under study, the operation of the ELEC is determined by the existence of surplus energy that will not be possible to store in the BSS ($SOC_{bat}(k) \leq \overline{SOC_{bat}}$), the operation of the FC is determined by the existence of energy deficit that will not be possible to be supplied by the BSS ($SOC_{bat}(k) \geq \underline{SOC_{bat}}$ and $SOC_{bat}^{end} \geq SOC_{bat}^{ini}$), see Figs. 6, 8–10.

Their operating conditions are characterised by start-up and shut-down processes subject to the constraints in the power variations $\Delta P_{ch/dis_{H2}}$ imposed, if applicable, Fig. 8 (case 2) and 9 (case 3). Likewise, the MPC controller promotes their smooth operation at stable operating power, as far as possible, especially in case 1 (Fig. 6) where C_i^{degr} is considered. In case 2, this operation is also observed due to fixed costs (it is more economical to switch on the system for the shortest possible time), see Fig. 8. On the contrary, this effect is not so clearly observed in case 3, where slightly more fluctuating performance profiles are observed in the ELEC, see Fig. 9. Finally, in the particular case of case 4, the HBSS power is adapted by turning on and/or off an integer number of ELECs and FCs according to the nominal power of each device, see Fig. 10, during the intervals 4 h $\leq t \leq$ 6 h, 8 h $\leq t \leq$ 9:20 h, 10.6 h $\leq t \leq$ 18:30 h and 19:20 h $\leq t \leq$ 22 h. Again, it is shown that for all cases the SOC_{H2} evolve and comply with the limits imposed by the constraints, see Figs. 6, 8-10.

Regarding the use of the MEG, in case of energy surplus, its use is reduced exclusively to the sale of surplus energy when the SOCs of the HESS has reached the maximum level (or it is not necessary to store more energy for later use). This operation is justified because, according to the defined cost terms, it is always more profitable to store energy in the HESS for later use than to sell energy and then purchase it from the MEG. For example, this can be seen in Fig. 8, case 2, 12:30 h $\leq t \leq$ 13:30 h and 17 h $\leq t \leq$ 19 h.

In case of energy deficit, the use of the MEG is promoted during the night hours with the lowest associated energy purchase cost (22 h $\leq t \leq$ 24 h, according to Table 10). Even, if it is of interest to the microgrid, the purchase of energy for the BSS charging process is considered (interval 22 h $\leq t \leq$ 24 h in the Figs. 6, 9-10) with a double purpose: 1) to take advantage of the BSS during the least economic hours, 2) to satisfy the final SOC_{bat} constraint. Also, MEG is used as a last resort, regardless of energy cost, when the HESS will not be able to cope energy deficits, in order to ensure power balance according to (5). For example, this can be seen in Fig. 6 during the interval 24 h $\leq t \leq$ 1 h; Fig. 8 during the interval 20.5 h $\leq t \leq$ 22 h (must be met $SOC_{bat}^{end} \leq SOC_{bat}^{ini} = 90\%$); Fig. 9 during the intervals 5 h $\leq t \leq$ 8 h, 9 h $\leq t \leq$ 10 h and 22 h $\leq t \leq$ 4 h; and Fig. 10 during the intervals 6 h $\leq t \leq$ 8 h, 9 h $\leq t \leq$ 10 h and 22 h $\leq t \leq$ 3 h.

Finally, although it is not the aim of the paper to provide an economic analysis for each case, as expected, and according to Table 11, it is shown that the cost obtained by the MPC-based EMS $Cost_{MPC}$, regardless of the architecture or application of the microgrid, allows considerable reductions in operating costs. $Cost_{MPC}$ (and the cost based on self-consumption without ESS, $Cost_{ren}$) are compared to the costs obtained with the traditional solution with exclusive connection to the MEG $Cost_{MEG}$. MPC-based EMS costs between 10% and 37% of the $Cost_{MEG}$ (90% and 63% reduction respectively). $Cost_{ren}$ has costs between 23.5% and 59% of the $Cost_{MEG}$ (76.5% and 41% reduction respectively).

Based on the coherent results obtained, it is demonstrated that regardless of the microgrid architecture, bus integration method, ESS used or application, the proposed modelling methodology and subsequent design phase of MPC controllers allows addressing the problem of technical-economic optimisation in energy management in microgrids with guarantees and in an easy and intuitive way.

5. Conclusions

The design of EMS for microgrid energy management is a fundamental task to achieve the different technical and economic objectives in a safe and efficient way. In this sense, MPC-based controllers have proven to be comprehensive solutions by integrating concepts such as prediction or optimality. Specifically, in the case of microgrids, the main advantage of MPC is that it allows to optimise the current situation without losing sight of future situations.

Since the microgrid concept nowadays encompasses a multitude of architectures and applications, it is essential to have general MPC-based EMSs that allow their application in different situations with only slight variations in their formulation. However, most of the solutions proposed in the scientific literature are specific to the model or design of the optimisation problem for each case under study and, therefore, cannot be extrapolated to other different cases.

This lack of generalisation detected when addressing the problem of optimal control of microgrids has been the motivation for this work. Thus, this article presents a general methodology for the design of state-space Economic MPC controllers for microgrid control regardless of their architecture, application or design objectives. The main objective of this approach was to simplify and systematise the MPC-based EMS design process from the initial modelling phase to the subsequent definition of the optimisation problem.

In order to evaluate the goodness of the proposed controller design approach, simulations have been performed for different scenarios, namely four microgrid architectures and applications with completely different generation and demand profiles. The results obtained are promising and the main conclusion that can be drawn is that the design

methodology and controller architecture presented in this work allows the design of EMSs for the control of microgrids in a systematized way, by means of simple guidelines.

The limitations of the proposed work have to do with its implementation in real-time. The computational cost of solving an MPC with low sampling periods is high. Therefore, it is proposed as a future work to adapt the proposed methodology for its implementation in real-time. For this purpose, it is proposed, for example, the implementation using a hierarchical MPC. In this type of control, the upper level corresponds to the MPC obtained through the methodology proposed in this work.

CRediT authorship contribution statement

A. Pajares: Writing – original draft, Validation, Software, Methodology, Investigation, Formal analysis, Conceptualization. **F.J. Vivas:** Writing – original draft, Software, Methodology, Investigation, Formal analysis, Conceptualization. **X. Blasco:** Writing – review & editing, Supervision, Project administration, Methodology, Investigation. **J.M. Herrero:** Writing – review & editing, Supervision, Project administration, Methodology, Conceptualization. **F. Segura:** Writing – review & editing, Supervision, Investigation, Conceptualization. **J.M. Andújar:** Writing – review & editing, Supervision, Project administration, Conceptualization.

Declaration of Competing Interest

The authors declare that they have no known competing financial interests or personal relationships that could have appeared to influence the work reported in this paper.

Data availability

Data will be made available on request.

Acknowledgements

This work was supported in part by grant PID2020-116616RB-C31 and grant PID2021-124908NB-I00 founded by MCIN/AEI/10.13039/501100011033 and by “ERDF A way of making Europe”; by the Generalitat Valenciana regional government through project CIAICO/2021/064, by Andalusian Regional Program of R + D + i (P20- 00730), and by the project “The green hydrogen vector. Residential and mobility application”, approved in the call for research projects of the Cepsa Foundation Chair of the University of Huelva.

References

[1] Vivas FJ, Heras A De Las, Segura F, Andújar JM. A review of energy management strategies for renewable hybrid energy systems with hydrogen backup. Renew Sustain Energy Rev Feb. 2018;82:126–55. https://doi.org/10.1016/J.RSER.2017.09.014.

[2] Caparrós Mancera JJ, et al. Experimental analysis of the effects of supercapacitor banks in a renewable DC microgrid. Appl Energy Feb. 2022;308:118355. https://doi.org/10.1016/J.APENERGY.2021.118355.

[3] Heras A De Las, Vivas FJ, Segura F, Andújar JM. From the cell to the stack. A chronological walk through the techniques to manufacture the PEFCs core. Renew Sustain Energy Rev Nov. 2018;96:29–45. https://doi.org/10.1016/J.RSER.2018.07.036.

[4] Brik K, Ben Ammar F. Causal tree analysis of depth degradation of the lead acid battery. J Power Sources Apr. 2013;228:39–46. https://doi.org/10.1016/J.JPOWSOUR.2012.10.088.

[5] Benmouna A, Becherif M, Depernet D, Gustin F, Ramadan HS, Fukuhara S. Fault diagnosis methods for proton exchange membrane fuel cell system. Int J Hydrogen Energy Jan. 2017;42(2):1534–43. https://doi.org/10.1016/J.IJHYDENE.2016.07.181.

[6] Velarde P, Maestre JM, Ocampo-Martinez C, Bordons C. Application of robust model predictive control to a renewable hydrogen-based microgrid. In: 2016 European control conference, ECC 2016; Jan. 2017. p. 1209–14. https://doi.org/10.1109/ECC.2016.7810454.

[7] Bordons C, García-Torres F, Valverde L. Gestión Óptima de la Energía en Microrredes con Generación Renovable. Revista Iberoamericana de Automática e Informática Industrial RIAI Apr. 2015;12(2):117–32. https://doi.org/10.1016/J.RIAI.2015.03.001.

[8] Blasco X, Martínez M, Herrero JM, Ramos C, Sanchis J. Model-based predictive control of greenhouse climate for reducing energy and water consumption. Comput Electron Agric Jan. 2007;55(1):49–70. https://doi.org/10.1016/J.COMPAG.2006.12.001.

[9] Bordons C, Garcia-Torres F, Ridao MA. Model predictive control of microgrids. 2020. https://doi.org/10.1007/978-3-030-24570-2.

[10] Mbungu NT, Ismail AA, AlShabi M, Bansal RC, Elnady A, Hamid AK. Control and estimation techniques applied to smart microgrids: a review. Renew Sustain Energy Rev Jun. 01, 2023;179. https://doi.org/10.1016/j.rser.2023.113251. Elsevier Ltd.

[11] Castilla M, Bordons C, Visioli A. Event-based state-space model predictive control of a renewable hydrogen-based microgrid for office power demand profiles. J Power Sources Feb. 2020;450:227670. https://doi.org/10.1016/J.JPOWSOUR.2019.227670.

[12] Torreglosa JP, García P, Fernández LM, Jurado F. Energy dispatching based on predictive controller of an off-grid wind turbine/photovoltaic/hydrogen/battery hybrid system. Renew Energy Feb. 2015;74:326–36. https://doi.org/10.1016/J.RENENE.2014.08.010.

[13] Velarde P, Valverde L, Maestre JM, Ocampo-Martinez C, Bordons C. On the comparison of stochastic model predictive control strategies applied to a hydrogen-based microgrid. J Power Sources Mar. 2017;343:161–73. https://doi.org/10.1016/J.JPOWSOUR.2017.01.015.

[14] Vivas Fernández FJ, Manzano FS, Márquez JMA, Calderón Godoy AJ. Extended model predictive controller to develop energy management systems in renewable source-based smart microgrids with hydrogen as backup. theoretical foundation and case study. Sustainability Oct. 2020;12(21):8969. https://doi.org/10.3390/SU12218969.

[15] Garcia-Torres F, Zafra-Cabeza A, Silva C, Grieu S, Darure T, Estanqueiro A. Model predictive control for microgrid functionalities: review and future challenges. Energies Feb. 2021;14(5):1296. https://doi.org/10.3390/EN14051296.

[16] Hu J, Shan Y, Guerrero JM, Ioinovici A, Chan KW, Rodriguez J. Model predictive control of microgrids – an overview. Renew Sustain Energy Rev Feb. 2021;136:110422. https://doi.org/10.1016/J.RSER.2020.110422.

[17] Torreglosa JP, García-Triviño P, Fernández-Ramirez LM, Jurado F. Control based on techno-economic optimization of renewable hybrid energy system for stand-alone applications. Expert Syst Appl Jun. 2016;51:59–75. https://doi.org/10.1016/J.ESWA.2015.12.038.

[18] Garcia F, Bordons C. Optimal economic dispatch for renewable energy microgrids with hybrid storage using model predictive control. In: IECON proceedings (industrial electronics conference); 2013. p. 7932–7. https://doi.org/10.1109/IECON.2013.6700458.

[19] Kou P, Liang D, Gao L. Distributed EMPC of multiple microgrids for coordinated stochastic energy management. Appl Energy Jan. 2017;185:939–52. https://doi.org/10.1016/J.APENERGY.2016.09.092.

[20] Pan X, Niu X, Yang X, Jacquet B, Zheng D. Microgrid energy management optimization using model predictive control: a case study in China. IFAC-PapersOnLine Jan. 2015;48(30):306–11. https://doi.org/10.1016/J.IFACOL.2015.12.395.

[21] Garcia-Torres F, Bordons C. Optimal economical schedule of hydrogen-based microgrids with hybrid storage using model predictive control. IEEE Trans Ind Electron Aug. 2015;62(8):5195–207. https://doi.org/10.1109/TIE.2015.2412524.

[22] Garcia-Torres F, Bordons C, Ridao MA. Optimal economic schedule for a network of microgrids with hybrid energy storage system using distributed model predictive control. IEEE Trans Ind Electron Mar. 2019;66(3):1919–29. https://doi.org/10.1109/TIE.2018.2826476.

[23] Vivas FJ, Segura F, Andújar JM, Calderón AJ, Isorna F. Battery-based storage systems in high voltage-DC bus microgrids. A real-time charging algorithm to improve the microgrid performance. J Energy Storage Apr. 2022;48:103935. https://doi.org/10.1016/J.EST.2021.103935.

[24] Garcia-Torres F, Valverde L, Bordons C. Optimal load sharing of hydrogen-based microgrids with hybrid storage using model-predictive control. IEEE Trans Ind Electron Aug. 2016;63(8):4919–28. https://doi.org/10.1109/TIE.2016.2547870.

[25] Vivas FJ, Segura F, Andújar JM, Caparrós JJ. A suitable state-space model for renewable source-based microgrids with hydrogen as backup for the design of energy management systems. Energ Conver Manage Sep. 2020;219:113053. https://doi.org/10.1016/J.ENCONMAN.2020.113053.

[26] G SM Mousavi, Nikdel M. Various battery models for various simulation studies and applications. Renew Sustain Energy Rev Apr. 2014;32:477–85. https://doi.org/10.1016/J.RSER.2014.01.048.

[27] Tremblay O, Dessaint LA, Dekkiche AI. A generic battery model for the dynamic simulation of hybrid electric vehicles. In: VPPC 2007 - Proceedings of the 2007 IEEE vehicle power and propulsion conference; 2007. p. 284–9. https://doi.org/10.1109/VPPC.2007.4544139.

[28] Copetti JB, Lorenzo E, Chenlo F. A general battery model for PV system simulation. Progress Photovolt Res Appl Oct. 1993;1(4):283–92. https://doi.org/10.1002/PIP.4670010405.

[29] Pajares A, Blasco X, Herrero JM, Simarro R. Non-linear robust identification of a lead acid battery model using multiobjective evolutionary algorithms. IFAC-PapersOnLine Jul. 2017;50(1):4466–71. https://doi.org/10.1016/J.IFACOL.2017.08.375.

[30] Argyrou MC, Christodoulides P, Marouchos CC, Kalogirou SA. Hybrid battery-supercapacitor mathematical modeling for PV application using Matlab/Simulink. In: Proceedings - 2018 53rd International universities power engineering conference, UPEC 2018; Nov. 2018. https://doi.org/10.1109/UPEC.2018.8541933.

[31] Wang Y, et al. A comprehensive review of battery modeling and state estimation approaches for advanced battery management systems. Renew Sustain Energy Rev Oct. 2020;131:110015. https://doi.org/10.1016/J.RSER.2020.110015.
[32] Pajares A, Blasco X, Herrero JM, Simarro R. Using a multiobjective approach to compare multiple design alternatives—an application to battery dynamic model tuning. Energies Jul. 2017;10(7):999. https://doi.org/10.3390/EN10070999.
[33] Palma-Behnke R, et al. A microgrid energy management system based on the rolling horizon strategy. IEEE Trans Smart Grid 2013;4(2):996–1006. https://doi.org/10.1109/TSG.2012.2231440.
[34] Khodaei A. Microgrid optimal scheduling with multi-period islanding constraints. IEEE Trans Power Syst 2014;29(3):1383–92. https://doi.org/10.1109/TPWRS.2013.2290006.
[35] Yang P, Nehorai A. Joint optimization of hybrid energy storage and generation capacity with renewable energy. IEEE Trans Smart Grid 2014;5(4):1566–74. https://doi.org/10.1109/TSG.2014.2313724.
[36] Jiang Q, Xue M, Geng G. Energy management of microgrid in grid-connected and stand-alone modes. IEEE Trans Power Syst 2013;28(3):3380–9. https://doi.org/10.1109/TPWRS.2013.2244104.
[37] Malysz P, Sirouspour S, Emadi A. An optimal energy storage control strategy for grid-connected microgrids. IEEE Trans Smart Grid 2014;5(4):1785–96. https://doi.org/10.1109/TSG.2014.2302396.
[38] Mendes PRC, Maestre JM, Bordons C, Normey-Rico JE. A practical approach for hybrid distributed MPC. J Process Control Jul. 2017;55:30–41. https://doi.org/10.1016/J.JPROCONT.2017.01.001.
[39] Anuphappharadorn S, Sukchai S, Sirisamphanwong C, Ketjoy N. Comparison the economic analysis of the battery between lithium-ion and lead-acid in PV stand-alone application. Energy Procedia Jan. 2014;56(C):352–8. https://doi.org/10.1016/J.EGYPRO.2014.07.167.
[40] Mongird K, et al. An evaluation of energy storage cost and performance characteristics. Energies Jun. 2020;13(13):3307. https://doi.org/10.3390/EN13133307.
[41] Zakeri B, Syri S. Electrical energy storage systems: a comparative life cycle cost analysis. Renew Sustain Energy Rev Feb. 2015;42:569–96. https://doi.org/10.1016/J.RSER.2014.10.011.
[42] Petrollese M, Valverde L, Cocco D, Cau G, Guerra J. Real-time integration of optimal generation scheduling with MPC for the energy management of a renewable hydrogen-based microgrid. Appl Energy Mar. 2016;166:96–106. https://doi.org/10.1016/J.APENERGY.2016.01.014.
[43] Castañeda M, Cano A, Jurado F, Sánchez H, Fernández LM. Sizing optimization, dynamic modeling and energy management strategies of a stand-alone PV/hydrogen/battery-based hybrid system. Int J Hydrogen Energy Apr. 2013;38(10):3830–45. https://doi.org/10.1016/J.IJHYDENE.2013.01.080.
[44] Pajares A, Blasco X, Herrero JM, Simarro R. Multivariable controller design for the cooling system of a PEM fuel cell by considering nearly optimal solutions in a multiobjective optimization approach. Complexity 2020;2020. https://doi.org/10.1155/2020/8649428.
[45] Vivas FJ, Heras A De Las, Segura F, Andújar JM. Cell voltage monitoring all-in-one. A new low cost solution to perform degradation analysis on air-cooled polymer electrolyte fuel cells. Int J Hydrogen Energy 2019;44(25):12842–56. https://doi.org/10.1016/j.ijhydene.2018.12.172.
[46] "https://www.idae.es/".
[47] "https://www.ree.es/es".
[48] Naderi E, Bibek KC, Ansari M, Asrari A. Experimental validation of a hybrid storage framework to cope with fluctuating power of hybrid renewable energy-based systems. IEEE Trans Energy Convers Sep. 2021;36(3):1991–2001. https://doi.org/10.1109/TEC.2021.3058550.
[49] DOE. EV everywhre grand challenge - battery status and cost reduction prospects. 2012.
[50] Akhil AA, et al. SANDIA REPORT 2013 electricity storage handbook in collaboration with NRECA. 2013.
[51] A. E. M. Commission. Future energy storage trends: An assessment of the economic viability, potential uptake and impacts of electrical energy storage on the NEM 2015–2035. 2015.
[52] Kazim A. Exergoeconomic analysis of a PEM fuel cell at various operating conditions. Energ Conver Manage May 2005;46(7–8):1073–81. https://doi.org/10.1016/J.ENCONMAN.2004.06.036.
[53] Kazim AM. Exergoeconomic analysis of a PEM electrolyser at various operating temperatures and pressures. Int J Energy Res May 2005;29(6):539–48. https://doi.org/10.1002/ER.1073.
[54] Duman AC, Güler Ö. Techno-economic analysis of off-grid PV/wind/fuel cell hybrid system combinations with a comparison of regularly and seasonally occupied households. Sustain Cities Soc Oct. 2018;42:107–26. https://doi.org/10.1016/J.SCS.2018.06.029.
[55] DOE. Fuel cell technologies program record 12020: Fuel cell system cost - 2012. 2012.
[56] Bemporad A, Morari M. Control of systems integrating logic, dynamics, and constraints. Automatica Mar. 1999;35(3):407–27. https://doi.org/10.1016/S0005-1098(98)00178-2.
[57] Mignone D, Bemporad A, Morari M. Framework for control, fault detection, state estimation, and verification of hybrid systems. In: Proceedings of the American control conference. 1; 1999. p. 134–8. https://doi.org/10.1109/ACC.1999.782755.